

**Examining the Effects of Soil Moisture on *Carex aquatilis* Productivity in a Saline  
Reclaimed Fen in the Athabasca Oil Sands Region**

by

Sarah Mohammad

A thesis

presented to the University of Waterloo

in fulfilment of the

thesis requirement for the degree of

Master of Science

in

Geography

Waterloo, Ontario, Canada, 2024

© Sarah Mohammad 2024

### **Author's Declaration**

I hereby declare that I am the sole author of this thesis. This is a true copy of the thesis, including any required final revisions, as accepted by my examiners. I understand that my thesis may be made electronically available to the public.

## Abstract

The Nikanotee fen is an experimental, constructed peatland in the region, established as a research site to develop strategies for future reclamation projects. Its main challenges include poor water quality caused by elevated salinity levels, which pose significant risks to the survival of its vegetation community. *Carex aquatilis* (*C.aquatilis*), a species of particular interest, is notable for its ability to tolerate diverse hydrochemical conditions, including high sodium concentrations. This study aimed to evaluate the effects of soil moisture on various chlorophyll fluorescence and gas exchange productivity parameters of *C.aquatilis* in the saline environment of the Nikanotee fen, with the goal of providing insights for its potential use in future reclamation projects in the AOSR. Through the use of a portable photosynthesis system, daily measurements of chlorophyll fluorescence ( $F_v/F_m$ ,  $F_v'/F_m'$ , and  $\phi$ PSII) and gas exchange parameters ( $E$ ,  $a$ , and  $A_{max}$ ) were conducted to monitor the effects of soil moisture and water table depth in the varying moisture plots on *C.aquatilis*. The findings of this study determined that while varying moisture levels may not directly impact the productivity of *C.aquatilis*, they could influence its stress responses by enabling the species to develop adaptations suited to the surrounding moisture conditions. This is demonstrated by the statistically significant decreases in the stress ratio ( $F_v/F_m$ ) during the heat wave observed in *C.aquatilis* grown in the 'Moderate' moisture plot compared to those in the 'Dry' and 'Wet' plots. Additionally, this study revealed that *C.aquatilis* may employ different salt tolerance mechanisms depending on moisture conditions. Plants grown in the 'Wet' moisture plots exhibited a higher sodium concentration in their aboveground biomass than in their belowground biomass compared to those in the 'Dry' and 'Moderate' plots, while still maintaining a statistically significantly higher  $\phi$ PSII and  $A_{max}$  values. These results demonstrate the resilience of *C.aquatilis* and its ability to sustain essential productivity levels for survival in increasingly reclaimed saline wetlands, such as the Nikanotee Fen.

## **Acknowledgements**

First and foremost, I would like to express my deepest gratitude to my supervisor, Dr. Richard Petrone. I am truly grateful to have had the opportunity to work with you and to be part of the Hydrometeorology Lab. Throughout my graduate studies, you have been incredibly patient and supportive, while always encouraging me to think critically about my work. Your guidance has been essential to the completion of my thesis, and I will always be thankful for your mentorship.

I would also like to thank everyone in the Hydrometeorology Lab and the Fort McMurray crew for the invaluable guidance throughout this journey. Special thanks go to Myroslava Khomik, Adam Green, Nataša Popovic, Brandon Van Huizen, Olena Volik, Abby Wang, Eric Murray, Suyuan Yang, and Sarah Fettah. I am also deeply grateful to Tianshi Wang for being the best fieldwork partner, offering constant support through the challenges of working under COVID-19 restrictions, and still bringing laughter to our days.

I would like to extend my heartfelt thanks to my family and friends. I am especially grateful for my mother and father, who have always encouraged me to work hard and strive to be the best version of myself, while supporting and loving me in every decision I make. My siblings, Thuraya and Ahmed, have also been invaluable throughout this journey, always there to help and contributing greatly to my successes. I owe particular gratitude to my beloved husband, Ali, for his unwavering support through the late nights and for always being my biggest fan yet offering constructive criticism when needed. His love and encouragement have been instrumental throughout this process, and I am deeply thankful to have him in my life.

## **Land Acknowledgements**

I would like to acknowledge that my thesis's lab and desk work takes place at the University of Waterloo, which is situated on the Haldimand Tract, land promised to the Six Nations, including six miles on each of the Grand River. I would like to acknowledge that my thesis's field research takes place within the boundaries of Treaty 8, traditional lands of the Dene and Cree, as well as the traditional lands of the Métis of northeastern Alberta.

## Table of Contents

Author’s Declaration.....	ii
Abstract.....	iii
Land Acknowledgements.....	v
List of Figures.....	vii
List of Tables.....	ix
Chapter 1. Introduction and Literature Review.....	1
1.1. Introduction.....	1
1.2. Literature Review.....	6
1.2.1. Wetlands in the Western Boreal Plain and the Athabasca Oil Sands Region.....	6
1.2.2. Chlorophyll Fluorescence Overview.....	12
Chapter 2. Methodology.....	18
2.1. Study Site and Plot Selection.....	18
2.2. MET Tower Data.....	23
2.3. Soil Moisture and Water Table Depth Measurements.....	24
2.4. Chlorophyll Fluorescence and Gas Exchange Measurements.....	25
2.4.1. Dark-Adapted Fluorescence Measurements ( $F_v/F_m$ ).....	27
2.4.2. Light-Adapted Fluorescence Measurements ( $F_v'/F_m'$ , $\phi$ PSII).....	28
2.4.3. Light Response Curves ( $A_{max}$ ) Measurements.....	29
2.5. Belowground and Aboveground Biomass Collection and Analysis.....	30
2.6. Statistical Analyses.....	31
Chapter 3. Results.....	33
3.1. Variations in Soil Moisture and Water Table Depth.....	33
3.2. Variations in Chlorophyll Fluorescence and Gas-Exchange Analyses.....	36
3.2.1. Chlorophyll Fluorescence ( $F_v/F_m$ , $F_v'/F_m'$ , and $\phi$ PSII).....	36
3.2.2. Gas-Exchange (Transpiration, Carbon Assimilation, and Light-Response Curves).....	41
3.3. Variations in Salinity of Belowground, Aboveground, and Litter Biomass.....	48
Chapter 4. Discussion.....	54
4.1. The Role of Edaphic Conditions on <i>Carex aquatilis</i> Productivity Parameters ...	54
4.1.1. Seasonal Variability in Edaphic Conditions.....	54
4.1.2. Chlorophyll Fluorescence.....	56
4.1.3. Transpiration, Carbon Assimilation, and Light Response Curves.....	63
4.2. Impacts of Salinity on the Overall Productivity of <i>Carex aquatilis</i> .....	69
4.2.1. Litter, Aboveground, and Belowground Biomass Sodium Concentration.....	69
Chapter 5. Conclusion.....	74
References.....	79

## List of Figures

**Figure 2-1** Map of the Nikanotee fen located 40 km north of Fort McMurray, Alberta (56°55.944’N, 111°25.035 W) with the key landmarks and the experimental plots used in this study identified (created by Nataša Popovic, 2023). The yellow dots represent the ‘Dry’, the blue dots represent the ‘Wet’, and the green dots represented the ‘Moderate’ experimental plots where the main productivity, gas exchange, moisture and salinity parameters were measured. ....21

**Figure 2-2 (a)** Photo of the set-up for the ‘Dry’ experimental plot. Location for the ‘Dry’ plots had no visual standing water and the *C.aquatilis* stalks were completely exposed. **(b)** Photo of the set up for the ‘Wet’ experimental plot. Location for the ‘Wet’ plots had high levels of standing water, with the *C.aquatilis* stalks mostly submerged. **(c)** Photo of the ‘Moderate’ experimental plot that acted as a control site. Location for the ‘Moderate’ plots had low levels of standing water and the *C.aquatilis* stalks were not completely submerged or exposed. ....22

**Figure 2-3.** The three graphs depict meteorological data collected by the MET tower through the field season of the experiment from the day of the year (DOY) 173 to 243. The top bar graph demonstrates the total sum of precipitation measured in millimetres. The middle line graph illustrates the average temperature recorded during the field season. The bottom line graph exhibits the average PAR values observed throughout the field season.....23

**Figure 2-4.** Photos of the overall set-up for the dark-adapted measurements. **a)** The photo demonstrates how each plot was dark-adapted using a black tarp for at least 30 minutes prior to beginning any measurements. **b)** The photo demonstrates how the dark-adapted measurements were conducted by removing the tarp and placing the *C.aquatilis* stalks within the gasket of the LI-6800, allowing the flash could be initiated through the console. ....28

**Figure 3-1.** Violin plots for **a)** the average daily volumetric water content (VWC) measured in July and August 2021 for the ‘Dry’, ‘Moderate’, and ‘Wet’ plots; and **b)** measured water table depth (WTD) in July and August 2021 for the ‘Dry’, ‘Moderate’, and ‘Wet’ plots. Black dots represent daily VWC and WTD measurements for that specific plot condition. Red dot represents the monthly mean of the VWC and WTD. ....34

**Figure 3-2.** Violin plots in **a)** show the daily  $F_v/F_m$  ratio and in **b)**  $F_v'/F_m'$  ratio measured in July and August 2021 for the dark-adapted *Carex aquatilis* within the ‘Dry’, ‘Moderate’, and ‘Wet’ plots. Black dots indicate the daily measurements of that variable for each replicate in

that specific moisture condition. The red dot represents the monthly mean of the data for that moisture condition. In plot **a)** The shaded green area signifies the approximate range (0.75+) in which plants are known to be typically healthy and unstressed .....38

**Figure 3-3.** Violin plot demonstrating the daily  $\phi$ PSII value measured in July and August 2021 for the light-adapted *Carex aquatilis* within the ‘Dry’, ‘Moderate’, and ‘Wet’ plots. Black dots indicate the daily  $\phi$ PSII measurements for each replicate within that specific moisture condition. The red dot represents the monthly mean of the  $\phi$ PSII data for that moisture condition. ....39

**Figure 3-4.** Violin plot demonstrating the daily dark and light transpiration rate ( $\text{mm s}^{-1}$ ) of the *Carex aquatilis* plants measured in July and August 2021 within the ‘Dry’, ‘Moderate’, and ‘Wet’ plots. Black dots indicate the daily transpiration rate for each replicate within that plot. The red dot represents the monthly mean of the transpiration rate data for that moisture condition. ....43

**Figure 3-5.** Violin plot displaying the daily dark and light carbon assimilation rate ( $\mu\text{mol m}^{-2} \text{s}^{-1}$ ) of the *Carex aquatilis* plants measured in July and August 2021 within the ‘Dry’, ‘Moderate’, and ‘Wet’ plots. Black dots indicate the daily assimilation rate for each replicate within that plot. The red dot represents the monthly mean of the assimilation rate data for that plot condition. ....44

**Figure 3-6.** Violin plot illustrating the maximum photosynthetic capacity at saturating light levels ( $A_{\text{max}}$ ) ( $\mu\text{mol CO}_2 \text{ m}^{-2} \text{ s}^{-1}$ ) of the *Carex aquatilis* plants measured in July and August 2021 within the ‘Dry’, ‘Moderate’, and ‘Wet’ plots. Black dots indicate the  $A_{\text{max}}$  rate for each specific plant replicate within each plot. The red dot represents the monthly mean of the  $A_{\text{max}}$  data for that moisture condition. ....45

**Figure 3-7.** Violin plot illustrating the belowground biomass sodium concentration ( $\text{mg/kg}$ ) of the *Carex aquatilis* plants in 0-10 cm, 10-30 cm, and 30-50 cm soil levels within the ‘Dry’, ‘Moderate’, and ‘Wet’ plots. Black dots indicate the sodium concentration for each specific replicate within each plot. The red dot represents the mean of the sodium concentration data for that moisture condition.....50

**Figure 3-8.** Violin plot illustrating the aboveground and litter biomass sodium concentration ( $\text{mg/kg}$ ) of the *Carex aquatilis* plants within the ‘Dry’, ‘Moderate’, and ‘Wet’ plots. Black dots indicate the sodium concentration for each specific replicate within each plot. The red dot represents the mean of the sodium concentration data for that moisture condition. ....51

## List of Tables

**Table 3-1.** Average volumetric water content (%) (n=53) and water table depth (cm) (n=51) ( $\pm$  standard deviation) for the ‘Dry’, ‘Moderate’, and ‘Wet’ plots within the Nikanotee Fen in July and August 2021.....35

**Table 3-2.** Kruskal-Wallis and Wilcoxon signed-rank test for the volumetric water content (%) and water table depth (cm) within the ‘Dry’, ‘Moderate’, and ‘Wet’ plots in July and August 2021. Note that \*, \*\*, \*\*\*, and \*\*\*\* indicate significance at 0.05, 0.01, <0.001, and <0.0001, respectively.....35

**Table 3-3.** Average stress ratio ( $F_v/F_m$ ), operating efficiency of PSII under light conditions ( $F_v'/F_m'$ ), and quantum yield of PSII under light conditions ( $\phi$ PSII) ( $\pm$  standard deviation) of *Carex aquatilis* plants in the ‘Dry’, ‘Moderate’, and ‘Wet’ plots within the Nikanotee fen in July and August 2021, n=109. ....40

**Table 3-4.** Kruskal-Wallis and Wilcoxon signed-rank test for the  $F_v/F_m$ ,  $F_v'/F_m'$ , and  $\phi$ PSII results within the ‘Dry’, ‘Moderate’, and ‘Wet’ plots in July and August 2021. Note that \*, \*\*, \*\*\*, and \*\*\*\* indicate significance at 0.05, 0.01, <0.001, and <0.0001, respectively and ns indicates not significant.....40

**Table 3-5.** Average transpiration ( $E$ ) ( $\text{mm s}^{-1}$ ) (n=109), carbon assimilation ( $a$ ) ( $\mu\text{mol m}^{-2} \text{s}^{-1}$ ) (n=109), and maximum photosynthetic capacity at saturating light levels ( $A_{max}$ ) ( $\text{CO}_2 \text{ m}^{-2}\text{s}^{-1}$ ) (n=78) ( $\pm$  standard deviation) of *Carex aquatilis* plants in the ‘Dry’, ‘Moderate’, and ‘Wet’ plots within the Nikanotee fen in July and August 2021. ....46

**Table 3-6.** Kruskal-Wallis test for transpiration ( $E$ ) ( $\text{mm s}^{-1}$ ), carbon assimilation ( $a$ ) ( $\mu\text{mol m}^{-2} \text{s}^{-1}$ ), and light assimilation rate of carbon assimilation ( $A_{max}$ ) ( $\text{CO}_2 \text{ m}^{-2}\text{s}^{-1}$ ) results within the ‘Dry’, ‘Moderate’, and ‘Wet’ plots in July and August 2021. Note that \*, \*\*, \*\*\*, and \*\*\*\* indicate significance at 0.05, 0.01, <0.001, and <0.0001, respectively and ns indicates not significant. ....46

**Table 3-7.** Wilcoxon signed-rank test for transpiration ( $E$ ) ( $\text{mm s}^{-1}$ ), carbon assimilation ( $a$ ) ( $\mu\text{mol m}^{-2} \text{s}^{-1}$ ), and light assimilation rate of carbon assimilation ( $A_{max}$ ) ( $\text{CO}_2 \text{ m}^{-2}\text{s}^{-1}$ ) results within the ‘Dry’, ‘Moderate’, and ‘Wet’ plots in July and August 2021. Note that \*, \*\*, \*\*\*, and \*\*\*\* indicate significance at 0.05, 0.01, <0.001, and <0.0001, respectively and ns indicates not significant.....47

**Table 3-8.** Average ( $\pm$  standard deviation) belowground biomass sodium concentrations of the *Carex aquatilis* plants at depths of 0-10cm (n =12), 10-30cm (n =12), and 30-50cm (n

=12) within the ‘Dry’, ‘Moderate’, and ‘Wet’ plot conditions in the Nikanotee fen, August 2021.....52

**Table 3-9.** Average ( $\pm$  standard deviation) aboveground (n=12) and litter (n=12) biomass sodium concentrations of the *Carex aquatilis* plants within the ‘Dry’, ‘Moderate’, and ‘Wet’ plot conditions in the Nikanotee fen, August 2021.....52

**Table 3-10.** Kruskal-Wallis and Wilcoxon signed-rank test for the belowground biomass sodium concentration in the *Carex aquatilis* plants at depths of 0-10 cm, 10-30 cm, and 30-50 cm under the ‘Dry’, ‘Moderate’, and ‘Wet’ plot conditions in the Nikanotee fen, August 2021. Note that \*, \*\*, \*\*\*, and \*\*\*\* indicate significance at 0.05, 0.01, <0.001, and <0.0001, respectively and ns indicates not significant.....52

**Table 3-11.** Kruskal-Wallis and Wilcoxon signed-rank test for the aboveground and litter biomass sodium concentration in the *Carex aquatilis* plants under the ‘Dry’, ‘Moderate’, and ‘Wet’ plot conditions in the Nikanotee fen, August 2021. Note that \*, \*\*, \*\*\*, and \*\*\*\* indicate significance at 0.05, 0.01, <0.001, and <0.0001, respectively and ns indicates not significant.....53

\

## **Chapter 1. Introduction and Literature Review**

### **1.1. Introduction**

The Athabasca Oil Sands Regions (AOSR) contains the world's largest bitumen deposits (Government of Alberta, 2020). Since 1857, these bitumen deposits have been the site for many extraction projects (Government of Alberta, n.d.). While only 5% of the bitumen deposits are accessible for surface mining, the majority are buried at depths that require drilling wells for extraction (Government of Alberta, n.d.). Techniques used for bitumen extraction are often invasive, involving the excavation of key ecosystems within the AOSR, such as peatlands and forests (Rooney & Bayley, 2011). Peatlands are indispensable ecosystems that provide major contributions to the environment, including water storage, vegetation growth, peat formation, carbon sequestration and biodiversity (Biagi et al., 2019). As a result of these open-pit mining projects, approximately 1055 km<sup>2</sup> of peatlands have been impacted (Alberta Environment and Parks, 2020). In response to the impact of these vital biomes, the Government of Alberta has implemented the Environmental Protection and Enhancement Act, which outlines the requirements for the reclamation of these sites (Rooney & Bayley, 2011). These areas must be restored to a state that is similar, although not necessarily identical, to their pre-disturbance state in which they can sustain a complex ecosystem (Rooney & Bayley, 2011). However, the process of reclamation is often complex, sensitive, and encompasses several drawbacks that prevent the complete restoration of these landscapes. Key issues include adapting these fens to reflect the region's future climatic conditions and preserving water quality in an environment with limited water resource (Ketcheson et al., 2016).

In the AOSR, the Nikanotee Fen is an experimental reclamation site used for conducting research and studies on the long-term functionality of reclaimed peatlands (Ketcheson et al., 2016). The fen itself is a pioneering attempt, created through years of modelling work to

accurately reflect the complex hydrological and climatic conditions documented through previous restoration literature (Ketcheson et al., 2016; Price et al., 2010). The Nikanotee Fen, situated within a large 32 ha watershed bordered by both reclaimed and natural slopes, and supports various vascular vegetation that promotes peat development (Ketcheson et al., 2016; Price et al., 2010). The moisture conditions of the fen are directly dependent on the discharge from an adjacent upland aquifer and runoff from adjoining slopes (Kessel et al., 2018; Ketcheson et al., 2016). The upland aquifer, constructed from tailing sands, supplies the groundwater necessary to maintain water levels essential for peat formation within the fen (Kessel et al., 2018). Due to their abundance, tailing sands are often repurposed in reconstructed landscapes (Kessel et al., 2018). Tailing sands, by products of the bitumen extraction process, contain residual sodium and other toxic chemicals (Purdy et al., 2005).. Their harmful hydrochemical properties such as residual levels of sodium, can negatively impact water quality, vegetation, and soil within the fen, particularly during the early years following construction (Kessel et al., 2018). As a result, the management and monitoring of experimental sites like the Nikanotee Fen are essential, as reclaimed wetlands are planned to be constructed on previously disturbed mined sites that contain high levels of sodic and toxic chemicals (Vitt et al., 2020). These experimental sites provide crucial data for the future construction of other wetlands, but they are at risk as wetland vegetation cannot tolerate elevated levels of salinity (Vitt et al., 2020). Specifically, many wetland plants undergo significant stress, resulting in structural changes and an inability to maintain essential physiological functions required for growth and survival (Vitt et al., 2020). Over time, sustained levels of elevated salinity can completely inhibit the growth of peat-forming species, ultimately leading to their eventual loss from the ecosystem (Kessel et al., 2018; Vitt et al., 2020). To prevent this loss, research is required to explore the threshold and responses of various wetland species to salt stress within these novel ecosystems.

Previous laboratory experiments have quantified the threshold of saline exposure at which death occurs in typical wetland vegetation, such as *Typha*, *Beckmannia*, and *Carex* (Vitt et al., 2020). A common wetland species of great interest that has demonstrated resistance to elevated salinity conditions is *Carex aquatilis* (*C.aquatilis*), also known as water sedge (Koropchak et al., 2012, Vitt et al., 2020). *C.aquatilis* is a perennial sedge species abundant in the boreal peatlands of North America (Koropchak et al., 2012). *C.aquatilis* plants possess an adventitious rooting system enabling them to aggressively colonize different landscapes (Koropchak et al., 2012). While *C.aquatilis* plants range in height from 15 to 150 cm, they produce rhizomatous shoots twice a year, with a lifespan ranging from 12 to 18 months (Koropchak et al., 2012). Mature shoots of *C. aquatilis* develop flowers during the spring and summer months and typically undergo senescence in the fall (Koropchak et al., 2012). Based on previous research and global data available, *C.aquatilis* has a range of tolerance to variable hydrochemical conditions like pH (3.0-8.5), conductivity (0-8822  $\mu\text{s cm}^{-1}$ ), and Calcium ( $\text{Ca}^{+2}$ ) concentrations (0.2-146.6  $\text{mg L}^{-1}$ ) (Koropchak et al., 2012). Furthermore, recent experimentation has demonstrated that *C.aquatilis* is capable of tolerating sodium ( $\text{Na}^{+}$ ) concentrations up to 1079  $\text{mg L}^{-1}$ , and only beyond these levels do they exhibit reduced structural and functional performance (Vitt et al., 2020). The ability of *C.aquatilis* to tolerate a broad range of extreme conditions, especially salinity, makes it an effective species to introduce into reconstructed wetlands in the AOSR (Koropchak et al., 2012, Vitt et al., 2020).

The Nikanotee fen experimental site incorporated salt-tolerant species like *C.aquatilis* during the development of the vegetation community to mitigate the negative effects of elevated salinity levels (Ketcheson et al., 2016). While this reclaimed site has not yet reached salinity levels near the thresholds of vascular wetland species like *C.aquatilis*, the gradual rise in sodium concentrations within certain parts of these peatlands are approaching those limits (Vitt et al., 2020). Specifically, recent fieldwork has shown that within the Nikanotee fen, the

salinity threshold ( $300 \text{ mg L}^{-1}$ ) for common peat-forming moss species such as *Byrum* and *Tomenthypnum* was exceeded across the majority of the water surface (Yang et al., 2022). These saline conditions and their negative effects on non-vascular species are only amplified in combination with other important ecological factors that affect the fen such as moisture conditions and water levels (Yang et al., 2022). The construction of these reclaimed sites and the placement of specific non-vascular and vascular peat-forming species must be carefully calculated and considered (Yang et al., 2022). To ensure the success of future reclamation sites, additional data and research is required to explore the changes in productivity and structural attributes of these species, especially in resilient plants like *C.aquatilis*. To date, most research previously conducted with *C.aquatilis* is often carried out in controlled greenhouse environments, limiting the interaction of dynamic ecohydrological conditions that these species are exposed to within the AOSR. Further *in situ* experimentation is required to measure changes in *C.aquatilis* productivity to determine its limitations and potential mechanisms it may employ when exposed to stressors in a saline environment. This information could provide a more comprehensive understanding of *C.aquatilis* and other vital wetland vegetation, ensuring the survival of these species and the success of the overall ecosystem.

While vegetation productivity can be measured through various functional attributes such as rate of photosynthesis, stomatal conductance, and transpiration, the use of chlorophyll analysis is a novel technique that has allowed researchers to study the photosynthetic process of plants on a deeper level (Guidi et al., 2019; Vitt et al., 2020). Chlorophyll analysis allows for measurement of specific fluorescence parameters that provide insight into the working efficiency of the photosynthetic processes of a plant (Maxwell & Johnson, 2000). Many researchers have incorporated chlorophyll fluorescence into their experimental design to measure the effects of abiotic and biotic stressors on plants, as it offers non-invasive and accurate results (Maxwell & Johnson, 2000). With the development of instrumentation such as

portable photosynthesis systems and fluorometers, fluorescence data that was previously difficult to collect is now more readily available (Murchie & Lawson, 2013). The use of this instrumentation within reclaimed wetlands can provide a better understanding of the integrated responses that species like *C.aquaticus* undergo when exposed to different environmental conditions.

This study was conducted in the Nikanotee Fen to assess changes in productivity of *C.aquaticus* when exposed to varying soil moisture levels in a saline reconstructed peatland, using a portable photosynthesis system (LI-6800; LiCor Biogeoscience Ltd., Nebraska, USA). Specifically, the aim of this study was to investigate how *C.aquaticus* functions in a saline environment, alongside other fluctuating ecohydrological conditions like soil moisture and water table depth. The hydrological processes in peatlands are among the most important factors that influence the vegetation community and vary throughout the growing seasons (Yao et al., 2021). Therefore, by investigating how the productivity of *C. aquaticus* is impacted by these changing environmental conditions, insights into the functioning of their photosystems and potential mechanisms used to mitigate salt stress can be gleaned. This information is integral to the reclamation process as it provides guidance and suggestions when developing the composition of these vegetation communities. Additionally, it helps identify the ideal locations for planting based on moisture conditions and salinity levels. Therefore, the specific objectives of this thesis are to:

1. Assess the impacts of variable soil moisture on different fluorescence and gas productivity parameters of *Carex aquaticus* in the saline growing environment of the Nikanotee Fen.
2. Assess the overall productivity and functional capacity of *Carex aquaticus* within a saline environment, along with providing insights for future use of the species in reclamation projects in the AOSR.

## 1.2. Literature Review

### 1.2.1. Wetlands in the Western Boreal Plain and the Athabasca Oil Sands Region

The Western Boreal Plains (WBP) of Alberta, Canada consists of various landscapes ranging from shallow lakes, large wetlands, and extensive upland forests (Thompson et al., 2017). These diverse ecosystems fulfil vital ecological, social, and economic roles both locally and globally (Kennedy & Mayer, 2002). Consequently, the WBP has become a region for significant ecosystem disturbance as result of industrial urbanization, agriculture, and mineral extraction activities (Chasmer et al., 2016; Volik et al., 2020). Wetlands are crucial ecosystems because of the high productivity of their vegetation communities and important ecohydrological roles, serving as buffers between terrestrial and aquatic ecosystems (Kennedy & Mayer, 2002). Wetlands are characterized as areas saturated with water for a duration sufficient to support hydric soils, hydrophytic vegetation, and biological activity typical of a wet environment (Kennedy & Mayer, 2002). Within the WBP, these habitats typically consist of significant amounts of decomposed organic matter with low decomposition rates, strongly affected by hydrological and chemical factors in this subhumid climate region (Elmes & Price, 2019; Thompson et al., 2017). Wetlands are generally divided into five broad classes, extending from peatlands to marshes, which can be further subdivided based on specific water chemistry and hydrological characteristics unique to their location (ex. fens versus bogs) (Kennedy & Mayer, 2002). Additionally, naturally occurring saline wetlands are rare in the region, with only 10 such areas indentified within the WBP (Trites & Bayley, 2009; Volik et al., 2020). These wetlands often form near major river systems where groundwater discharges from saline aquifers, resulting in conditions that are slightly acidic to neutrally chloride dominated (Volik et al., 2020; Wells & Price, 2015). Saline wetlands often exhibit salinity gradients and differ from other natural wetlands due to their lower species richness in vegetation and the prevalence of salt-tolerant plants (Volik et al., 2020; Wells & Price, 2015). The unique interactions

between the salt-tolerant vegetation community and the abiotic conditions of these ecosystems are of significant interest in the field of reclamation (Volik et al., 2020; Wells & Price, 2015). This has been the focus of numerous studies, particularly as the increasing cation concentrations in these sites has gained importance in recent years (Vitt et al., 2020). Regardless of classification, wetlands play essential roles in physical, biological, and chemical processes both locally within the WBP and globally (Kennedy & Mayer, 2002).

Important functions of wetlands may encompass flood control, purification of contamination, enhancement of water quality, and substantial involvement in various biogeochemical cycles (Kennedy & Mayer, 2002). Peatlands are vital wetlands, wielding significant influence despite covering only 3% of the Earth's surface, largely due to their substantial capacity for carbon sequestration (Limpens et al., 2008). In peatlands, carbon sequestration occurs when carbon dioxide (CO<sub>2</sub>) is absorbed from the atmosphere and stored within the decomposed organic soil matter, known as peat (Were et al., 2019). Due to the waterlogged and anaerobic characteristics of peatlands, the decomposition process of organic soil matter slows down, preventing the release of carbon back into the atmosphere (Limpens et al., 2008; Were et al., 2019). Consequently, the carbon accumulates over time and becomes stored in the peat, effectively removing CO<sub>2</sub> from the atmosphere and serving as a carbon sink (Limpens et al., 2008; Were et al., 2019). The accumulation of peat and carbon uptake are significantly influenced by the hydrology of the system, as lower water table levels lead to increase oxygen availability which in turn enhances peat decomposition (Elmes & Price, 2019). Conserving these landscapes is essential, as any disturbance or drainage of peatlands can lead to the release of stored carbon back into the atmosphere, thereby contributing to greenhouse gas emissions (Limpens et al., 2008; Were et al., 2019). Additionally, abiotic factors, such as increased salinity levels in peatlands, may hinder carbon accumulation, as saline fens typically store less carbon compared to naturally occurring fens in the regions (Volik et al., 2018).

Among the diverse range of peatlands found within the AOSR, fens are the most prevalent type, demonstrating variations in richness depending on local hydrogeologic settings (Elmes & Price, 2019; Volik, Elmes, et al., 2020). In the AOSR, poor-fens typically form over areas where groundwater is recharged (Elmes & Price, 2019). These areas are characterized by fine-grained substrates that limit water movement across the landscape, restricting the replenishment of water within the peat and reducing nutrient availability (Elmes & Price, 2019). In contrast, rich-fens develop in areas where there is a flow of water, either from runoff or discharged groundwater (Elmes & Price, 2019). These areas are characterized by coarse-grained substrates that facilitate water movement, allowing nutrients to flow more readily (Elmes & Price, 2019). Groundwater exerts a significant impact on the ecological and biogeochemical functions of fens by altering water table levels and affecting water chemistry, influencing the overall biodiversity in the system (Elmes & Price, 2019). Alterations in water table levels can significantly influence carbon accumulation and carbon storage within fens (Elmes & Price, 2019). Lower water table levels indicate higher oxygen levels, leading to increased peat decomposition and decreased carbon accumulation (Elmes & Price, 2019). Conversely, higher water table levels slow peat decomposition, resulting in greater carbon accumulation and storage (Elmes & Price, 2019). Furthermore, groundwater discharge from adjacent uplands can help alleviate water stress and losses in fens during periods of low precipitation (Elmes & Price, 2019). Fens connected to intermediate flow groundwater systems receive discharge that travel longer distances, making them less susceptible to seasonal precipitation fluctuations, unlike those connected to shallow flow groundwater systems, which are more influenced by short-term precipitation patterns (Elmes & Price, 2019).

Within the AOSR, fens serve as crucial ecosystems integral to essential ecological and hydrological processes but are increasingly disturbed by bitumen extraction (Volik, Elmes, et al., 2020). Due to the presence of the world's largest bitumen deposits, the AOSR has become

a region for lucrative projects in the oil and gas industry, with investments totalling over \$21.6 billion in 2011 (Huang et al., 2016). The extraction of bitumen through open-pit mining is invasive and destructive, requiring the removal and excavation of entire landscapes to access the bitumen-rich McMurray Formation, thereby permanently altering key habitats. (Biagi et al., 2019). Oil sands mining operations overlay estuaries, marine sediment deposits, and saline aquifers, which are exposed during the mining process (Trites & Bayley, 2009). Consequently, the salts from these deposits and aquifers are released, leaching into various ecosystems and increasing salinity levels (Trites & Bayley, 2009). Subsequently, post-mining, excavated pits are refilled with waste materials known as tailings, notable for their heightened salinity (Biagi et al., 2019). The salinity of these tailings are attributed to exposed saline deposits and aquifers, as well as the use of chemicals such as caustic hot water (NaOH) and gypsum ( $\text{CaSO}_4 \cdot 2\text{H}_2\text{O}$ ) during the bitumen recovery process (Biagi et al., 2019). As a result, open-pit mining has caused disturbance to over 1055 km<sup>2</sup> of peatlands and forests within the AOSR (Alberta Environment and Parks, 2020). To mitigate the significant loss of these vital habitats, the Government of Alberta has implemented the Environmental and Enhancement Act, which requires industries to restore disturbed landscapes to a pre-disturbed state that can sustain a complex ecosystem after extraction (Biagi et al., 2019). Specifically, regulations mandate the reconstruction of forests and peatlands, notwithstanding the challenges and drawbacks inherent in the reclamation process (Biagi et al., 2019).

Creating reclaimed peatlands to replicate the natural hydrological and ecological functions of undisturbed peatlands is a complex and sensitive process with numerous challenges that demand extensive research and data (Biagi et al., 2019). One of the common challenges encountered during peatland reconstruction is the establishment of a hydrological regime capable of sustaining various ecosystem functions over an extended period (Biagi et al., 2019). Additionally, elevated salinity levels from by-products of open-pit mining pose a challenge, as

the salinity can inhibit vegetation growth and impede the succession necessary for long-term peatland development (Biagi et al., 2019). This process, which takes place over centuries, is driven by complex interactions of physical, chemical, and biological factors for peat development in these environments (Biagi et al., 2019). The reclamation process is further complicated by additional ongoing disturbances from human urbanization and refining practices within the region, as well as the threat of global warming (Volik et al., 2020). When designing a reclaimed system, it is essential to consider the region's climate, as factors like precipitation and evapotranspiration affect water availability, which is crucial for maintaining soil water storage and groundwater levels (Ketcheson et al., 2016). Despite the array of challenges, two experimental peatland systems have been constructed in the region to gain operational experience and develop strategies for future reclamation projects (Ketcheson et al., 2016). Particularly among these is the Nikanotee Fen, which serves as the study site for this experiment. The construction and design of the Nikanotee Fen were guided by a numerical modelling process, utilizing long-term climate data and vegetation threshold moisture conditions from previous reclamation literature (Price et al., 2010). The model integrated regional climate records from 1914 to 2004 and incorporated drought cycles of varying severity (Price et al., 2010). Subsequently, the numerical model was applied to the conceptual design of the fen to ensure that the hydrological conditions of the system could sustain the long-term survival of vegetation, particularly non-vascular mosses (Price et al., 2010). The revegetation strategy of the fen incorporated a diverse medley of native WBP wetland vegetation species including freshwater and saline sedges, graminoids, *Sphagnum*, and brown moss sourced locally from a nearby rich-fen (Borkenhagen & Cooper, 2019a; Ketcheson et al., 2016). The introduction of both vascular and non-vascular vegetation species enabled the formation and establishment of vegetation communities, thereby facilitating fen conditions (Ketcheson et al., 2016). Comparable to other reconstructed wetlands in the region, the Nikanotee Fen faces

similar challenges. These challenges include poor water quality due to elevated salinity levels resulting from solute transport into the fen from an upland aquifer formed by tailing waste materials (Ketcheson et al., 2016). The rise of salinization within the fen poses a significant risk to the survival vegetation communities, primarily due to the toxic effects on non-halophilic species (Ketcheson et al., 2016). While several modifications have been included in the construction of the Nikanotee Fen to mitigate increasing salinity levels, such as the inclusion of salt-tolerant plant species, the long-term survival of the vegetation community remains at risk (Ketcheson et al., 2016). Despite facing challenges, the success of the Nikanotee Fen remains subjective, yet the insights it has generated are invaluable for future site development within the AOSR (Ketcheson et al., 2016).

Over time, the Nikanotee Fen continues to serve as a focal point for research endeavours aimed at advancing the overall understanding of the reclamation process. Several experiments, conducted both in the field and laboratory, have been aimed at collecting data to address the ongoing challenges such as increasing salinity levels in the fen. Particularly, there has been a growing interest in salt-tolerant wetland vegetation species because of their resilience in adverse conditions. However, there is limited research exploring the mechanisms employed by these salt-tolerant species within the fen and the impact of salinization on their productivity. Further experimentation in the Nikanotee Fen is necessary to investigate the relationship between key wetland species and the influence of abiotic stressors such as salt on their overall functionality, and their role in the reclamation process. Recently, chlorophyll analysis has emerged as a ground-breaking technique for delving deeper into the productivity of wetland species, enabling researchers to evaluate the effects of stressors like salinity (Guidi et al., 2019). This technique permits the measurement of crucial fluorescence parameters, providing insights into the photosynthetic capabilities and mechanisms of plants (Murchie & Lawson, 2013).

### 1.2.2. Chlorophyll Fluorescence Overview

Chlorophyll fluorescence analysis has developed into a powerful technique used to investigate the photosynthetic performance of plants (Maxwell & Johnson, 2000). Since its discovery in the 1960's by Kautsky *et al.* (1960), the use of chlorophyll fluorescence in both laboratory and field studies has increased in frequency and popularity. These fluorescence parameters are often discussed in conjunction with multiple ecological variables that measure both plant health and productivity (Maxwell & Johnson, 2000). The underlying principle of chlorophyll fluorescence analysis involves light and the potential processes it undergoes once absorbed by a chlorophyll molecule within the leaves (Maxwell & Johnson, 2000). The processes occur due to changes in light energy that are closely tied to the reduction and oxidation state of electron carriers within the thylakoid membrane, where the majority of the light-dependent reactions occur (Maxwell & Johnson, 2000; Murchie & Lawson, 2013). When the leaf of a plant is exposed to sufficient levels of light to initiate photosynthesis after being in the dark for a significant period, there is a reduction in electron carriers in the thylakoid membrane (Murchie & Lawson, 2013). Specifically, P<sub>680</sub>, a special chlorophyll located within photosystem II (PSII) of plants, releases an electron to Quinone A (Q<sub>A</sub>), an electron acceptor (Murchie & Lawson, 2013). Q<sub>A</sub> cannot accept any more electrons from P<sub>680</sub> until it passes its electrons to the next carrier within the system, Quinone B (Q<sub>B</sub>) (Murchie & Lawson, 2013). Until then, the reaction centres within PSII are considered to be closed, resulting in an increase in the yield of chlorophyll fluorescence, also known as the re-emittance of light (Murchie & Lawson, 2013). Subsequent to this reduction of electrons and the elevation in chlorophyll fluorescence, there is an immediate decline in chlorophyll fluorescence yield within minutes (Maxwell & Johnson, 2000). This decrease in fluorescence yield levels occurs due to an increase in the number of electrons that travel away from PSII (Maxwell & Johnson, 2000). These electrons can be used to contribute to the overall photosynthetic and productivity

reactions within the plant through a process known as photochemical quenching (Maxwell & Johnson, 2000). However, these electrons can also be utilized to convert excess energy within the plant as heat, allowing it to dissipate from the plant to prevent the formation of free radicals in the system through a process known as non-photochemical quenching (Maxwell & Johnson, 2000). Photochemical and non-photochemical quenching, along with the increase in chlorophyll fluorescence yield, describe one of the three pathways that a chlorophyll molecule may take once exposed to light energy (Maxwell & Johnson, 2000). These three potential processes are in constant competition for excitation energy and are often interconnected, as the decrease in one results in an increase within the others (Maxwell & Johnson, 2000). By understanding the potential processes chlorophyll may undergo, they can be individually isolated to determine key information about the health and photosynthetic performance of a plant (Maxwell & Johnson, 2000).

The photosynthetic performance of a plant is typically determined through the measurements of chlorophyll fluorescence yield and inhibiting one of the quenching processes (Maxwell & Johnson, 2000). Initial experiments involved the use of pesticides to inhibit the photochemical quenching process within plants; however, this method proved to be impractical due to the irreversible damaging effects on plants (Baker, 2008). Eventually, with the advancement of technology, the development of portable photosynthesis systems that include fluorimeters were introduced (Baker, 2008). Fluorimeters contain modulating beams that release saturating flashes of light to induce low levels of chlorophyll fluorescence, which are measured and recorded within the instrument. Through this process, the instrument can calculate various fluorescence parameters that provide information about the photosynthetic efficiency and performance of a plant (Baker, 2008). Portable photosynthesis systems have enabled rapid quantitative data collection in both field and laboratory settings. These systems are non-detrimental and non-invasive to plants, yielding accurate results (Baker, 2008). While

the specifics of the modulating beam and the complexity of the device may differ from one instrument to another, the techniques and methods used to collect fluorescence variables are generally similar (Baker, 2008). Primarily, one of the most frequently measured variable is the maximum quantum yield of PSII photochemistry, noted as  $F_v/F_m$  (Baker, 2008). This value is calculated through the manipulation of a light energy source, which is done by dark-adapting an individual leaf or the entirety of a plant (Maxwell & Johnson, 2000). Dark-adapting occurs when the leaf or plant is physically blocked from an actinic light source long enough to ensure that the PSII centres are fully open, and no quenching processes occurred (Maxwell & Johnson, 2000). Through the attachment of the fluorometer onto the physical leaf of the plant, a modulated measuring beam is used to induce and record the minimum level of chlorophyll fluorescence ( $F_o$ ) (Maxwell & Johnson, 2000). However, the process used to induce  $F_o$  cannot be strong enough to stimulate electron transport and, consequently, photochemical quenching in PSII (Baker, 2008; Maxwell & Johnson, 2000). Once the  $F_o$  is recorded, the modulated measuring beam releases a series of short actinic light pulses to close the reaction centres within PSII and induce the maximum level of chlorophyll fluorescence ( $F_m$ ) (Baker, 2008; Maxwell & Johnson, 2000). The difference between  $F_o$  and  $F_m$  is used to calculate the value of variable fluorescence ( $F_v$ ), which in turn determines the  $F_v/F_m$  ratio (Baker, 2008; Maxwell & Johnson, 2000).  $F_v/F_m$  represents the maximum quantum yield of PSII photochemistry and is often known as the stress ratio. It provides an indication of the overall efficiency of PSII in converting absorbed light into chemical energy, as healthy and non-stressed plants exhibit consistent  $F_v/F_m$  values of approximately  $\sim 0.75$  and higher across a wide range of species (Baker, 2008; LICOR, 2022; Maxwell & Johnson, 2000). However, decrease in this value may suggest the presence of potential stressors impacting the efficiency of the plant PSII (Baker, 2008; Maxwell & Johnson, 2000).

In addition to measuring the  $F_v/F_m$  ratio, the actual quantum yield of PSII photochemistry ( $\phi$ PSII) is another variable that is also frequently assessed (Murchie & Lawson, 2013).  $\phi$ PSII provides insights into the amount of light energy that is absorbed and actually used in PSII photochemistry, considering variables such as light availability and energy partitioning within the photosynthetic apparatus of the plant (Murchie & Lawson, 2013). This parameter is measured through the exposure of a leaf or the entirety of a plant to a strong actinic light source for a period of time, known as light-adapting (Murchie & Lawson, 2013). The process of light-adapting causes a reduction of electrons, which may either be re-emitted as fluorescence or quenched photochemically or non-photochemically (Murchie & Lawson, 2013). Once the plant has reached stable levels with exposure to the light source, the fluorometer is physically attached to measure the steady-state level of fluorescence ( $F'$ ) (Murchie & Lawson, 2013). The modulated measuring beam releases brief saturating flashes of actinic light over a range of intensities and time, altering the  $F'$  and thereby closing the reaction centres within PSII (Murchie & Lawson, 2013). The fluorometer then calculates the maximum level of fluorescence ( $F_m'$ ) in the light-adapted state. This value typically yields a lower result compared to its dark-adapted counterpart,  $F_m$ , due to the contribution of photochemical and non-photochemical quenching processes that occur (Murchie & Lawson, 2013). The difference between  $F_m'$  and  $F'$  values are used to determine  $\phi$ PSII, which is also expressed as  $(F_m' - F')/F_m'$  (Murchie & Lawson, 2013). Typically, higher values of  $\phi$ PSII indicate a greater proportion of absorbed light energy effectively utilized in photochemical reactions by PSII (Olvera-González et al., 2013). Higher values of  $\phi$ PSII are often associated with healthier and active photosynthetic systems within plants, crucial for fostering plant growth and productivity (Baker, 2008). Additionally, as  $\phi$ PSII provides the value for the operating efficiency of PSII photochemistry, the rate of the electron transport can be computed using supplementary values

like photosynthetically active radiation (PAR) and the fraction of light used by PSI and PSII (Murchie & Lawson, 2013). Often  $\phi$ PSII is integrated with carbon fixation and assimilation parameters due to their linear relationship observed in laboratory settings (Murchie & Lawson, 2013). Both the  $F_v/F_m$  and  $\phi$ PSII parameters have garnered interest from various scientists across all disciplines of research due their simplicity in measurement and analysis. They are frequently incorporated in various studies to measure the responses of various plant species to abiotic and biotic stressors across multiple environments and settings (Xia et al., 2023).

Within the AOSR, the use of chlorophyll fluorescence analysis in the field is relatively new and limited, primarily reserved for agriculture research (Murchie & Lawson, 2013). Chlorophyll analysis techniques are often employed to screen for optimal plant traits by linking genomic information to phenological responses, with a focus on crop improvement (Murchie & Lawson, 2013). The demand for non-invasive, rapid, and accurate techniques to monitor photosynthesis performance has grown over the years, generating significant interest in using chlorophyll fluorescence analysis across various plant-related fields (Murchie & Lawson, 2013). Despite this growing interest, few studies have utilized  $F_v/F_m$  and  $\phi$ PSII parameters to monitor the productivity and efficiency of wetland vegetation in the region. Notably, Mollard et al. (2012) employed chlorophyll fluorescence analysis to investigate the physiological measurements of *C.aquaticus* grown in industrial, indirectly affected, and natural wetlands within the AOSR. By measuring  $F_v/F_m$  and other productivity parameters, Mollard et al. (2012) determined that despite reduced morphological size, *C.aquaticus*, demonstrated higher photochemical efficiency in industrial wetlands compared to unimpacted natural wetlands (Mollard et al., 2012). While these findings highlight the resilience of *C.aquaticus* in polluted areas of the AOSR and are promising for reclamation efforts, other key ecohydrological factors and stressors, such as fluctuating soil moisture levels, were not considered. Using chlorophyll analysis to monitor the productivity of *C.aquaticus* in the Nikanotee Fen under varying soil

moisture levels will provide a more dynamic understanding of the species' functionality in a reclaimed wetland. This approach considers the constantly changing environment the species is exposed to daily, offering deeper insights into its resilience and adaptive mechanisms when exposed to stressors.

## **Chapter 2. Methodology**

### **2.1. Study Site and Plot Selection**

This study was conducted within the fen landscape of the Nikanotee Fen Watershed (56°55.944'N, 111°25.035'W), located 40 km north of Fort McMurray, Alberta in an oil sands mining operation in the AOSR (Ketcheson et al., 2017). The Nikanotee Fen Watershed comprises an upland area (7.7 ha), a fen (2.2 ha), and surrounding slopes (18.7 ha), designed to facilitate the flow of groundwater from the upland to the fen in order to sustain a water table level at or near the surface (Kessel et al., 2018; Sutton & Price, 2020). Reclamation of the hillslopes was conducted in 2011 and contributes to the surface runoff that recharges the upland aquifer (Kessel et al., 2018; Sutton & Price, 2020). The uplands were constructed using a 2-3 m thick tailing sands aquifer on a 3% basal slope. An impermeable engineered geosynthetic clay liner was placed beneath, and a thin layer of salvaged forest floor soil was added on top. The fen portion of the watershed was constructed from approximately 2 m of moderately decomposed donor peat atop a layer of petroleum coke, measuring 0.5-0.7 m in depth. The petroleum coke layer extends 100 m into the uplands beneath the tailing sands layer, in a region referred to as the transition zone (Kessel et al., 2018; Sutton & Price, 2020). These specific materials were integrated into the construction of the watershed to facilitate the movement of water and solutes from the uplands into the fen (Kessel et al., 2018; Sutton & Price, 2020).

The high hydraulic conductivities among the layers of tailing sands and petroleum coke in the upland directs the lateral groundwater flow toward the petroleum coke underlayer (Kessel et al., 2018; Sutton & Price, 2020). In turn, this drives the groundwater flow towards the fen and upwards through the peat profile. Subsequently, flow exits the fen through a flume within a spill box positioned in the northeast corner of the fen where it enters an outflow pond (Figure 2-1). Groundwater flow from the upland maintains water table levels at or near the surface of the fen under drought conditions, while the reclaimed hillslopes contribute to runoff during the

spring freshet (Kessel et al., 2018; Sutton & Price, 2020). Vegetation in the fen was planted using a randomized split- box and split-split design, which included seedlings propagated in a commercial nursery and moss layer transfers. The moss layer transfer treatments consist of vegetation material that made up the top 0.05-0.1 m of moss. Additional moss, peat and vascular plants were collected from a nearby rich fen and spread at a ratio of 1:10, donor area to reclaimed area (Kessel et al., 2018; Murray et al., 2017). Currently, the vegetation community in the Nikanotee Fen includes a variety of vascular plants and bryophyte species (Borkenhagen & Cooper, 2019b). *Carex aquatilis* (*C.aquatilis*) is the most dominant vascular plant species, thriving across all hydrological gradients in the fen and producing more aboveground biomass than any other species (Borkenhagen & Cooper, 2019b). Additionally, vascular plants such as *Juncus balticus* serve as nurse plants and are commonly found in areas of the fen with high bryophyte richness, unlike the dense litter of *C.aquatilis*, which can inhibit bryophyte growth (Borkenhagen & Cooper, 2019b). Other species, such as *Typha latifolia* (*T.latifolia*), a marsh plant invasive to the fen, are commonly found in areas with near-surface water tables, specifically 0 to 10 cm below the soil surface (Borkenhagen & Cooper, 2019b). *T.latifolia* rapidly colonizes wet areas of the fen due to its high seed production and germination rates, raising concerns about its ability suppress essential peat-forming species (Borkenhagen & Cooper, 2019b). Consequently, *T.latifolia* was mechanically removed from the fen between 2015 to 2017, but are still found in inundated areas (Borkenhagen & Cooper, 2019b). In 2017, despite its low biomass, *Ptychostomum pseudotriquetrum* was the most common bryophyte in the fen and remains a crucial species due to its tolerance of saline conditions (Borkenhagen & Cooper, 2019b).

The experimental plots were selected within the fen and alongside the boardwalk to ensure easy access to the *C.aquatilis* plants for conducting productivity measurements (Figure 2-1). Three sets of plots were chosen based on visible soil moisture levels (dry, Moderate, wet) and

the availability of three *C.aquaticus* plants that were similar in age. Three replicate plots of each soil moisture condition were selected and measured. ‘Dry’ plots were selected in areas of the fen that contained no standing water and were completely dry (Figure 2-2a). The ‘Dry’ plots were located at the ends of the boardwalk, leading towards the uplands and the reclaimed hills of the watershed. ‘Wet’ plots were selected in areas of the fen where *C.aquaticus* stalks were completely submerged in water, and there were high levels of standing water (Figure 2-2b). ‘Moderate’ plots were selected as control experimental plots within the fen. ‘Moderate’ plots contained relatively low levels of standing water, but they were neither fully dry nor wet (Figure 2-2c). The experimental plots were all similar in size measuring approximately 1.2 m by 1.8 m. The plots were marked with wooden stakes at the corners and then connected using flagging tape (Figure 2-2). In each experimental plot, a well (constructed of PVC pipe), was installed in the centre for water sampling and water table depth measurements. Three *C.aquaticus* plant replicates were selected within each plot that were similar in age, size, and appearance. *C.aquaticus* plants that were flowering were avoided as they were older in age. Each plant was marked with a white flag, labelled ‘1’, ‘2’, and ‘3’ to ensure consistency when conducting productivity measurements throughout the season. Plants were labelled and recorded based on both soil moisture condition and flag number to differentiate between measurements (e.g., Dry 1: Plant 1, Plant 2, Plant 3 vs Dry 2: Plant 1, Plant 2, Plant 3). In early August, an additional set of ‘Dry’, ‘Wet’ and ‘Moderate’ experimental plots were added to the study, resulting in a total of four replicates for each soil moisture condition, with three *C.aquaticus* plants in each plots.

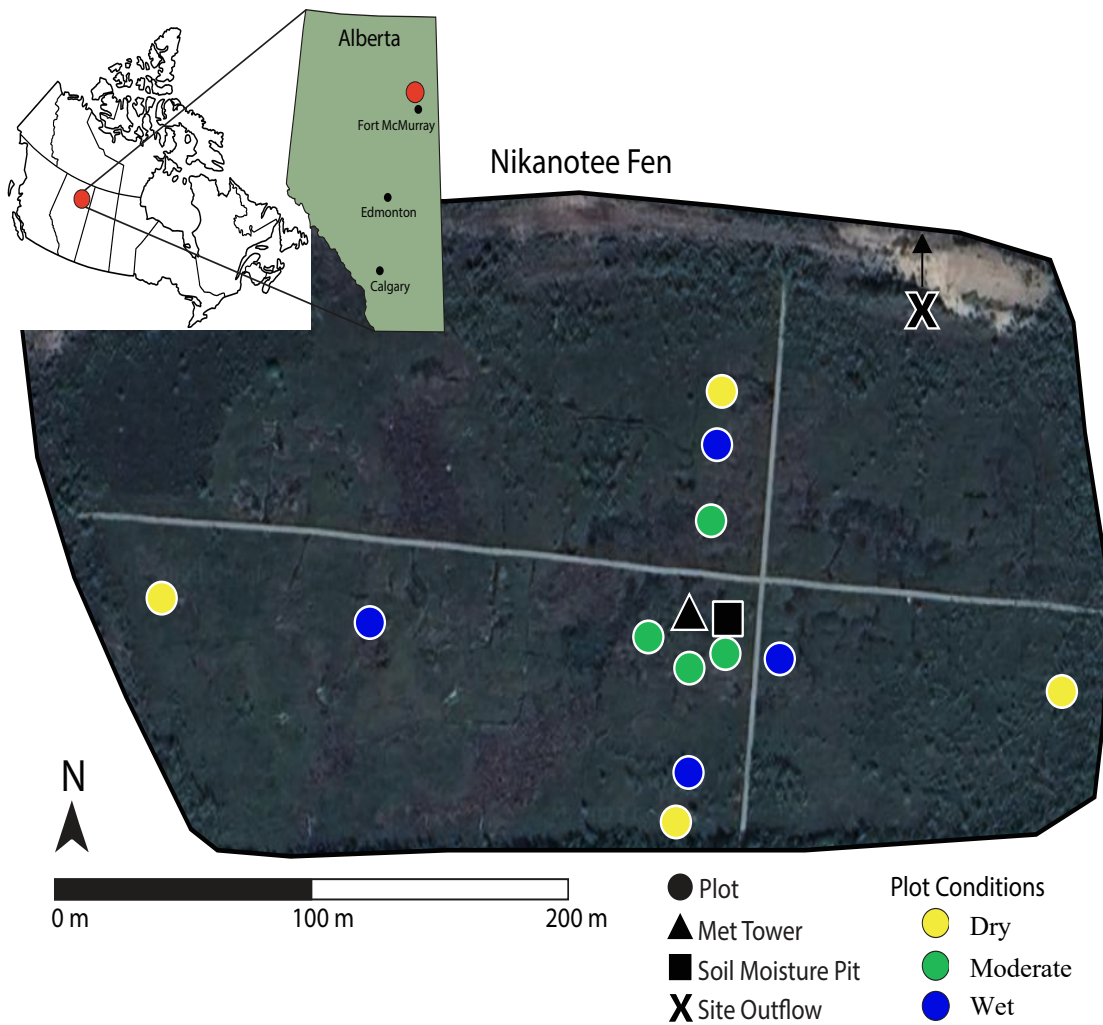


**Figure 2-1** Map of the Nikanotee fen located 40 km north of Fort McMurray, Alberta (56°55.944'N, 111°25.035 W) with the key landmarks and the experimental plots used in this study identified (created by Nataša Popovic, 2023). The yellow dots represent the 'Dry', the blue dots represent the 'Wet', and the green dots represented the 'Moderate' experimental plots where the main productivity, gas exchange, moisture and salinity parameters were measured.



**Figure 2-2 (a)** Photo of the set-up for the ‘Dry’ experimental plot. Location for the ‘Dry’ plots had no visual standing water and the *C.aquatilis* stalks were completely exposed. **(b)** Photo of the set up for the ‘Wet’ experimental plot. Location for the ‘Wet’ plots had high levels of standing water, with the *C.aquatilis* stalks mostly submerged. **(c)** Photo of the ‘Moderate’ experimental plot that acted as a control site. Location for the ‘Moderate’ plots had low levels of standing water and the *C.aquatilis* stalks were not completely submerged or exposed.

## 2.2. MET Tower Data

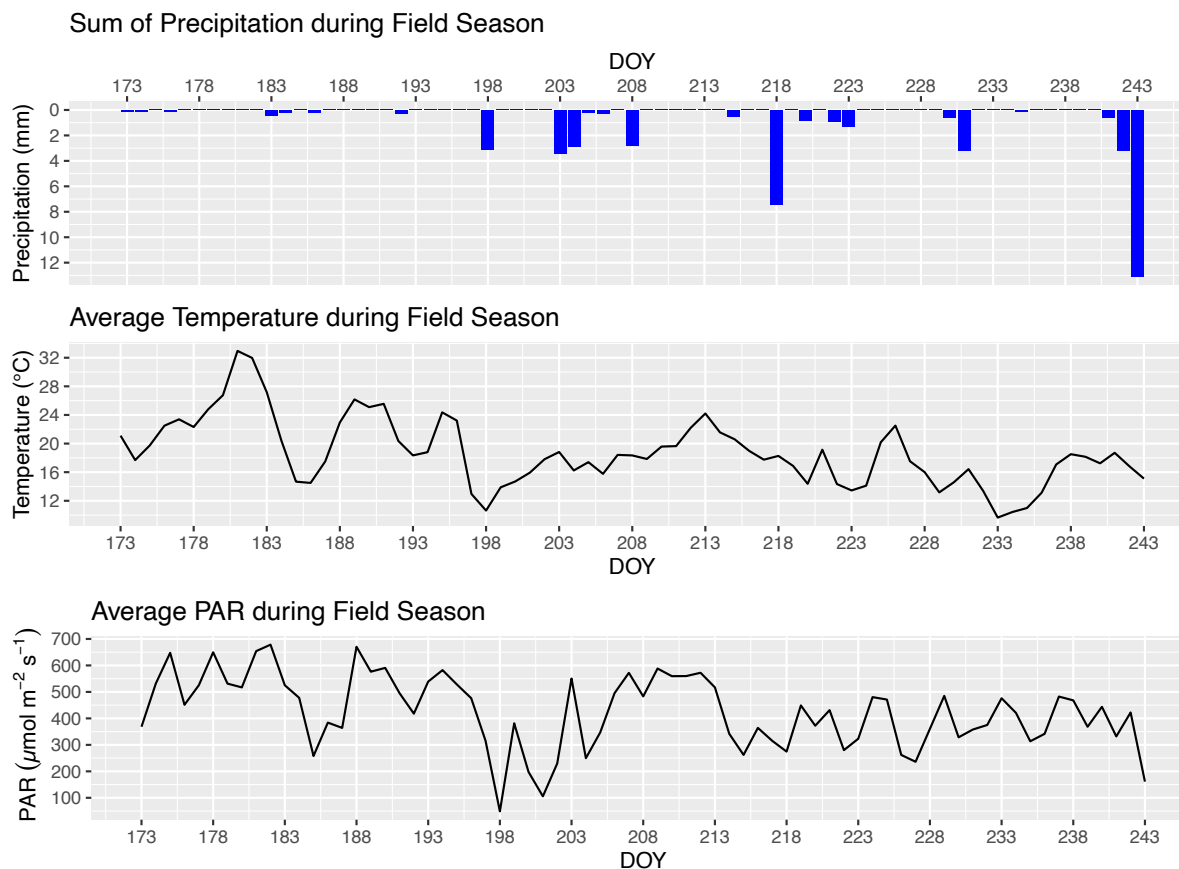


**Figure 2-3.** The three graphs depict meteorological data collected by the MET tower through the field season of the experiment from the day of the year (DOY) 173 to 243. The top bar graph demonstrates the total sum of precipitation measured in millimetres. The middle line graph illustrates the average temperature recorded during the field season. The bottom line graph exhibits the average PAR values observed throughout the field season.

Data for this study were collected from June 22<sup>nd</sup> to August 31<sup>st</sup>, 2021. At the onset of the field season, towards late June and early July, the region experienced an unusual spike in temperatures, with averages reaching a high of 32.9 °C (Figure 2-3). This heatwave set records across many regions in Western Canada, including Alberta (Environmental and Climate Change Canada, 2021). Historical data spanning three decades indicates that daily average temperature in Fort McMurray, Alberta, varied from 17.3°C in July and 15.6°C in August (Government of Canada, n.d.). In contrast, the average monthly temperature recorded by the meteorological tower were 19.4°C in July, and 16.5°C in August (Figure 2-3), surpassing the

historical daily averages in Fort McMurray. PAR levels exhibited a similar pattern to temperature, rising during the heatwave and gradually declining as the field season progressed (Figure 2-3). Precipitation events were initially infrequent at the beginning of the field season but gradually increased over time. The total monthly precipitation within the fen was 13.8 mm in July and 31.7 mm in August (Figure 2-3). In comparison, historical records spanning three decades show that precipitation in Fort McMurray, Alberta, ranged from 77.4 mm in July and 55.9 mm in August (Government of Canada, 2024). The recorded precipitation levels during the study were much lower in July and August compared to historical data, which demonstrated higher precipitation levels for these months. This suggests a relatively dry growing season, with precipitation only increasing towards the end of the measurement campaign in August.

### **2.3. Soil Moisture and Water Table Depth Measurements**

Soil moisture measurements were carried out daily before any fluorescence measurements using a Stevens HydraProbe and Hydra Data Reader (Stevens Water Monitoring Systems Inc., Oregon, USA). The prong (0.124 meters) of the HydraProbe was inserted into the soil of each experimental site and the readings displayed on the Hydra Reader (Voltage 1, Voltage 2, Voltage 3, Voltage 4, Temperature, Water Fractional Volume (FV), Loss Tangent, Soil Conductivity, Total Conductivity, Dielectric Constant/Current, and Temperature Compensation) were recorded. This process was repeated three times in three different locations within each plot.

Additionally, water table depth measurements were taken daily prior to any fluorescence measurements using the well installed in each experimental plot. A blow stick was used to measure water table levels within the PVC pipe. The outer measurement of the pipe was

subtracted from the inner measurement of the pipe to calculate the water table depth below the surface.

#### 2.4. Chlorophyll Fluorescence and Gas Exchange Measurements

Chlorophyll fluorescence, transpiration, and carbon assimilation measurements were conducted daily from late June to the end of August 2021. Measurements were conducted using the Li-Cor 6800 (LI-6800) Portable Photosynthesis System (LiCor Biosciences, Nebraska, USA). The LI-6800 uses a combination of gas analyzers and a fluorometer to concurrently measure gas exchange and fluorescence parameters. The LI-6800 employs an open gas exchange system to measure photosynthesis, carbon assimilation, and transpiration. It does this by assessing the changes in carbon dioxide and water content within the air stream that enters and exits the leaf cuvette within the chamber. The instrument provides automated mechanisms to adjust the concentrations of carbon dioxide and water in the incoming air, ensuring stable gas concentrations during fluorescence measurements. The instrument's fluorescence system includes a 'Multiphase Flash Fluorometer', which contains a light source and a chamber for conducting both gas exchange and fluorescence measurements. The aperture within the fluorometer was 6 cm<sup>2</sup>. The LI-6800 utilizes two different techniques to measure chlorophyll *a* fluorescence by employing different LEDs that serve distinct experimental functions and are used to calculate various fluorescence parameters. The first technique measures fluorescence emission using a pulse-amplitude modulation (PAM) fluorometer. The second technique quantifies the maximum fluorescence yield by applying a saturating flash of light. The PAM fluorometer itself provides a direct source of actinic modulated light, with the range of pulse and frequency varying based on the type of measurement. Pulses from the fluorometer have an approximate length of 1 microsecond, with frequency ranges spanning from 50 Hz to 250 kHz and a fixed amplitude of 100  $\mu\text{mol m}^{-2} \text{s}^{-1}$ . The modulated light within the PAM fluorometer

will emit pulses of fluorescence that are dim enough to avoid stimulating photosynthesis but will enable measurement of the quantum yield of fluorescence. The quantum yield of fluorescence will measure at values above zero to reflect the elicitation from the low pulses. However, once an actinic light source is applied in conjunction with the modulate light source, the flash will alter the redox photophysics of photosystem II (PSII) reaction centres, thereby altering the quantum yield of fluorescence and the rate constants for photosynthesis. The principles of calculating various photochemical parameters are dependent on photophysical processes that control the energy state of chlorophyll during photosynthesis. When conducting fluorescence measurements, the chlorophyll molecules are integrated into the LI-6800 and undergo various processes of de-excitation. These processes are associated with rate constants that are calculated and derived through various formulas and assumptions, leading to the measurement of the main fluorescence values. The specific derivations of these equations used to calculate these fluorescence parameters are described in detail within the LI-6800 Version 2 manual (LI-COR, 2022).

The LI-6800 contains three chemical columns connected to the console to ensure successful functionality of the instrument while conducting field measurements. The three chemical columns are the desiccant, humidifier, and carbon dioxide scrub column. The desiccant column contains Drierite to eliminate water vapour from the air when conducting measurements. The Drierite was regenerated as needed during the field season by placing it in an oven for 60 minutes at 210 °C, indicated by the beads changing from blue to pink in colour. The humidifier column contains Naifon tubing and water to humidify the air stream when conducting measurements. Filtered and room temperature water were added to the humidifier column as needed when water levels dropped below  $\frac{1}{4}$  of the column throughout the season. The carbon dioxide scrub column contains soda lime used to absorb and capture carbon dioxide from the air stream when conducting gas exchange measurements. The soda lime was regenerated as

needed by simply adding water, indicated by the pellets changing from white to violet in colour. The three columns were inspected every morning, and physical checks of the LI-6800 were conducted, along with a daily warm-up system test within the console (LI-COR, 2022).

Warm-up tests were carried out each day prior to any fluorescence or gas exchange measurements to ensure the system's functionality. During the warmup test, the infrared gas analyzers (IRGAs) were calibrated. The warm-up tests identified any potential issues with the instrument, and if any arose, they were addressed immediately before conducting any measurements. In addition, the stability criteria function within the console was utilized to monitor changes in carbon dioxide (CO<sub>2</sub>), fluorescence, humidity, and temperature during field measurements. Prior to initiating any measurements, 15 to 30 seconds were accounted for, and 3 out of 4 variables had to be stable. The LI-6800 was used in the fen peatland by securely attaching the console to a tripod and placing it either on the main boardwalk of the fen or directly within the fen area itself. Due to the instrument's sensitivity, fluorescence and gas exchange measurements were avoided during extreme weather conditions such as heavy rain and wind (LI-COR, 2022).

#### **2.4.1. Dark-Adapted Fluorescence Measurements ( $F_v/F_m$ )**

*C.aquaticus* plants within each experiment were dark-adapted using a large black tarp. The tarp was positioned over the three plants for a minimum of at least 30 minutes (Figure 2-4a). After the plants were completely dark-adapted, the tarp was quickly removed from the plant replicate being measured. Subsequently, the upper part *C.aquaticus* stalk was positioned flatly within the gasket ring of the head and then closed shut (Figure 2-4b). A hair clip was attached to the stalks of the plant to keep them flat and steady during measurements. Dark-adapted carbon assimilation and transpiration values were recorded simultaneously for each replicate once the flash was initiated. The measurement process was repeated between the three plant

replicates within each soil moisture plot ('Dry', 'Wet', and 'Moderate'). However, the tarp was not removed until the measurement of the previous replicate was completed to ensure the plants were not exposed to actinic light. Measurements were typically conducted from early morning to late afternoon (8:00 am to 3:00 pm) and were performed prior to any light-adapting measurements. Dark-adapted measurements were taken from the same transect for each experimental plot ('Dry 1', 'Wet 1', and 'Moderate 1') to ensure accurate comparisons could be made between the soil moisture conditions. Stalks that were similar in age and height were selected from each plant replicate to ensure consistency between measurements.



**Figure 2-4.** Photos of the overall set-up for the dark-adapted measurements. **a)** The photo demonstrates how each plot was dark-adapted using a black tarp for at least 30 minutes prior to beginning any measurements. **b)** The photo demonstrates how the dark-adapted measurements were conducted by removing the tarp and placing the *C. aquatilis* stalks within the gasket of the LI-6800, allowing the flash could be initiated through the console.

#### 2.4.2. Light-Adapted Fluorescence Measurements ( $F_v'/F_m'$ , $\phi$ PSII)

*C. aquatilis* plants within each soil moisture condition were light-adapted by exposing them to direct sunlight for a minimum of 30 minutes. The upper part of the *C. aquatilis* stalk was placed within the gasket and secured with a hair clip. Fluorescence levels on the console

screen were monitored, and upon the stabilization of the measurement criteria, the flash was initiated. Light-adapted carbon assimilation and transpiration values were recorded simultaneously for each replicate once the flash was initiated. The measurement process was repeated between the three plant replicates within each soil moisture condition ('Dry', 'Wet', and 'Moderate'). Measurements were conducted from late morning to late afternoon (11:00am to 4:00pm). Light-adapted measurements were taken from the same transect for each experimental plot ('Dry 1', 'Wet 1', and 'Moderate 1') to ensure accurate comparisons could be made between the soil moisture conditions. Stalks that were similar in age and height were selected from each plant replicate to ensure consistency between measurements.

#### **2.4.3. Light Response Curves ( $A_{max}$ ) Measurements**

Light response curves begin in complete darkness, where no photosynthesis is occurring within the leaf. When exposed to the first few photons of light, they are absorbed by the leaf, utilizing the maximum efficiency levels of its photosynthesis ability. As the light levels increase, the efficiency capabilities of the leaf decrease to a point at which the light energy will yield little to no increase in photosynthesis. Through the measurement of this process, a curve is generated which can provide insight into the light saturated rate of carbon assimilation ( $A_{max}$ ) and other variables (LI-COR, 2022).

The light response curve was conducted twice throughout the field season: first from July 15<sup>th</sup> to July 18<sup>th</sup>, 2021, and then a second time from August 18<sup>th</sup> to August 21<sup>st</sup>, 2021. Each light response curve took approximately one hour to generate, resulting in the completion of measurements for all replicates across all plots over multiple days. The light response curve is generated through an automated program in the console of the LI-6800 that progressively reduces the incident light released from the fluorometer (1680, 1260, 840, 670, 335, 165, 80, 60, 40, 20, 5, 0  $\mu\text{mol m}^{-2} \text{s}^{-1}$ ) to optimize quantum efficiency. All experimental plots were light-

adapted for a minimum of 30 minutes before to conducting the light response curves. The upper stalk of the *C.aquatilis* plant was positioned flatly within the gasket ring of the head and closed shut. A hair clip was attached to the stalks of the plant to keep them steady during measurements. The measurement process was repeated between the three plant replicates within each soil moisture condition ('Dry', 'Wet', and 'Moderate'). Measurements were conducted from early morning to late afternoon (8:00am to 3:00pm). Light curve response measurements were taken from the same transect for each experimental plot ('Dry 1', 'Wet 1', and 'Moderate 1') to ensure accurate comparisons could be made between the soil moisture conditions. Stalks that were similar in age and height were selected from each replicate to ensure consistency between measurements.

Light response curves were fitted using a non-linear least squares model, following the Levenberg-Marquardt (1978) algorithm:

$$A_{\text{net}} = A_{\text{max}} \left[ 1 - \left( 1 - \frac{R_d}{A_{\text{max}}} \right) \right]^{1 - \frac{\text{Par}}{\tau}} \quad (1)$$

where  $A_{\text{net}}$  ( $\mu\text{mol of CO}_2 \text{ m}^{-2} \text{ s}^{-1}$ ) is the net photosynthesis at a given light level (PAR  $\mu\text{mol m}^{-2} \text{ s}^{-1}$ ),  $A_{\text{max}}$  is the maximum photosynthetic capacity at saturating light levels ( $\mu\text{mol of CO}_2 \text{ m}^{-2} \text{ s}^{-1}$ ),  $R_d$  is the dark respiration rate of a leaf ( $\mu\text{mol of CO}_2 \text{ m}^{-2} \text{ s}^{-1}$ ), and  $\tau$  is the light compensation point. Data analysis was performed using the "Interface to the Levenberg-Marquardt Nonlinear Least-Square Algorithm Found in MINPACK, Plus Support for Bounds" package (Elzhov et al., 2016) within RStudio (Version 2023.09.1+494) (R Core Team, 2013).

## 2.5. Belowground and Aboveground Biomass Collection and Analysis

At the end of field season, on August 25<sup>th</sup>, 2021, both aboveground and belowground biomass samples were collected to analyse the presence and concentration of various chemical

elements, particularly sodium, using the ICP-OES technique. Within each soil condition, belowground biomass samples containing soil and roots were collected using a 50 cm-long soil corer made of PVC pipe. One soil core was collected from each experimental plot and split into three sections based on the depth below the surface: 0-10 cm, 10-30 cm and 30-50cm. Each section was placed in plastic Ziploc bags and stored in a freezer. Aboveground biomass samples were collected using 20x20 cm quadrat. The quadrat was positioned at the centre of the various plots, and the plant tissues were then harvested down to the soil surface using a clipper and placed in a paper bag. Subsequently, the aboveground biomass samples were dried in an oven at 60°C for 48 hours. Belowground samples were rinsed from the soil cores, and the root tissues were then placed in an oven and dried at 60°C for 48 hours. The dried plant tissue and roots were then taken to the Environmental Isotope Laboratory within the University of Waterloo. Here, they were ground using a ball mill (RETSCH M2, Germany) and stored in 5 mL vials. The vials were then sent to the Natural Resource Analytical Laboratory at the University of Alberta for chemical analysis. The samples were analyzed through the Thermo iCAP6300 Duo inductively coupled plasma-optical emission spectrometer (ICP-OES). A total of 12 elements were measured, however, the sodium concentration was main element required from this analysis.

## **2.6. Statistical Analyses**

The statistical computations and graphics for all collected data were performed using the R language within the integrated development environment, RStudio (Version 2023.09.1+494) (R Core Team, 2013). The Kruskal-Wallis test is a non-parametric test that is used to determine if there are statistically significant differences between two or more groups of an independent variable based on the relative rankings within the sample (Kruskal & Wallis, 1989). However, the Kruskal-Wallis test cannot distinguish which specific groups are statistically significant,

thus further statistical analyses were required (Kruskal & Wallis, 1989). To distinguish which variables were statistically significant, the Wilcoxon signed-rank test was utilized (Siegel, 1957). The Wilcoxon signed-rank test is a non-parametric equivalent of a t-test which was used to evaluate the significance of a variable under two or more different conditions (Siegel, 1957).

In this study, the data collected was non-parametrically distributed, so the Kruskal-Wallis test was used to determine whether there was statistically significant differences in the productivity variables measured for each experimental plot between the months of July and August. Subsequently, the Wilcoxon signed-rank test was then used to create pairwise comparisons between the different experimental plots for the various productivity measurements, determining their p-value and statistical significances.

## Chapter 3. Results

### 3.1. Variations in Soil Moisture and Water Table Depth

Throughout the study period, the experimental moisture plots ('Dry', 'Moderate', and 'Wet') exhibited seasonal and temporal variations in both soil moisture and water table depth (Figure 3-1). As indicated in Table 3-1, average volumetric water content (VWC) remained relatively consistent across all experimental plot types in both July and August. The 'Dry' plots displayed a lower VWC at approximately  $60 \pm 5.3$  %, followed by the 'Moderate' plots with an average of about  $69 \pm 4.4$  %, and the 'Wet' plots with the highest average VWC at around  $73 \pm 4.7$  %. The average water table depth (WTD) among the experimental plots showed slight variations between July and August. The 'Dry' plots demonstrated a lower average WTD, from  $-12.6 \pm 6.6$  cm in July to  $-9.2 \pm 6.8$  cm in August. Similarly, the 'Wet' plots and 'Moderate' plots also demonstrated an increase in the average WTD, rising from  $6.9 \pm 6.8$  cm to  $9.5 \pm 9.3$  cm and from  $0.6 \pm 6.2$  cm to  $2.1 \pm 6.6$  cm, respectively.

The Kruskal-Wallis test was utilized to identify statistically significant differences in both VWC and WTD in between the varying moisture plot, separating them into two seasons of the study: July and August (Table 3-2). The results revealed statistically significant differences for both WTD and VWC in both months, with p-values below 0.05. Subsequently, the Wilcoxon signed-rank test was conducted to determine significant differences among the pairwise comparison groups in both seasons. It was found that all pairwise groups, across all moisture conditions, exhibited statistically significant differences in both VWC and WTD for July and August, with p-values below 0.05 in all cases.

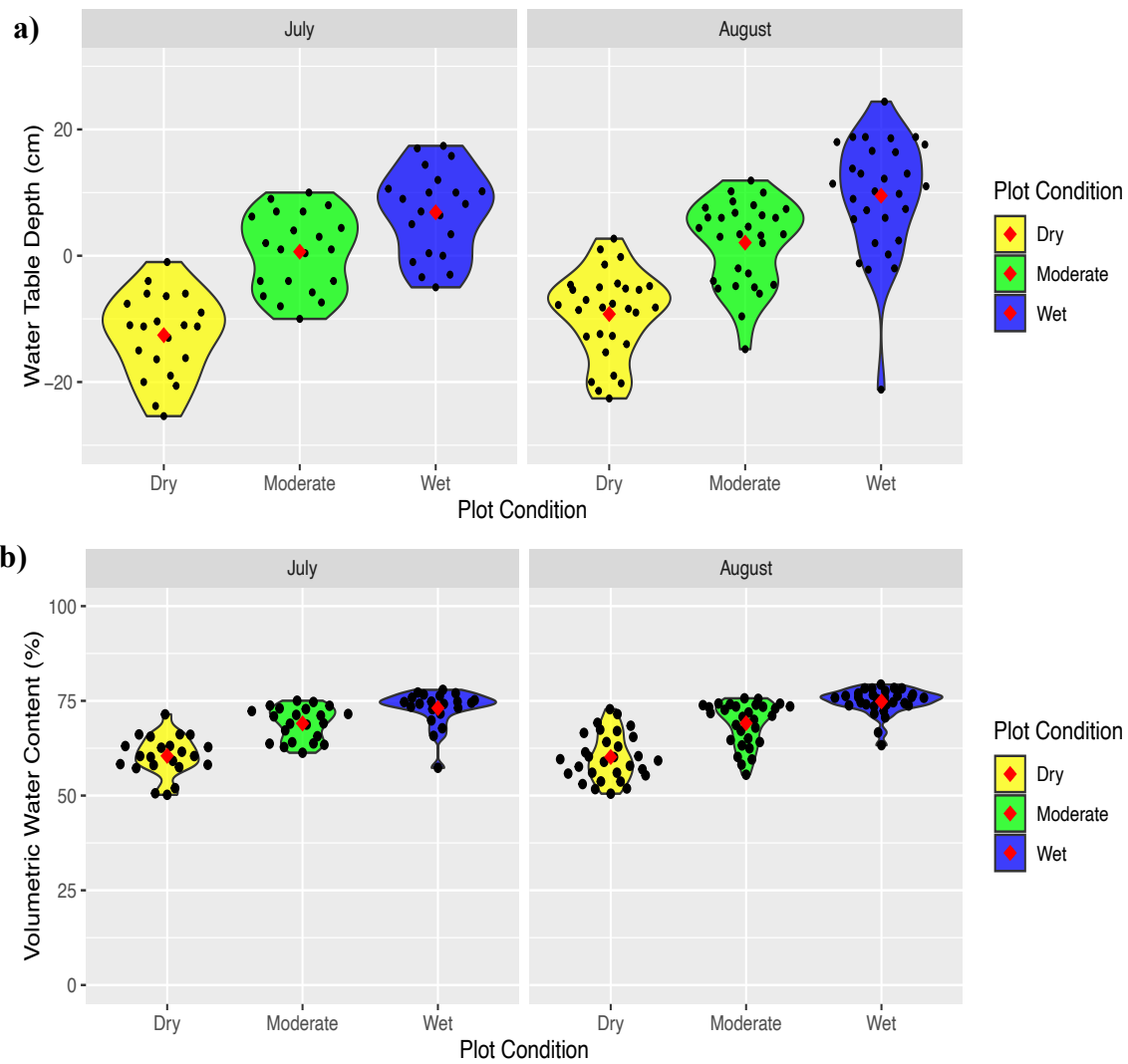


**Figure 3-1.** Violin plots for **a)** the average daily volumetric water content (VWC) measured in July and August 2021 for the ‘Dry’, ‘Moderate’, and ‘Wet’ plots; and **b)** measured water table depth (WTD) in July and August 2021 for the ‘Dry’, ‘Moderate’, and ‘Wet’ plots. Black dots represent daily VWC and WTD measurements for that specific plot condition. Red dot represents the monthly mean of the VWC and WTD.

**Table 3-1.** Average volumetric water content (%) (n=53) and water table depth (cm) (n=51) ( $\pm$  standard deviation) for the ‘Dry’, ‘Moderate’, and ‘Wet’ plots within the Nikanotee Fen in July and August 2021.

Month	Plot Condition	Avg VWC (%) $\pm$ SD	Avg WTD (cm) $\pm$ SD
July	Dry	60.5 $\pm$ 5.3	-12.6 $\pm$ 6.6
	Moderate	69.0 $\pm$ 4.4	0.6 $\pm$ 6.2
	Wet	73.1 $\pm$ 4.7	6.9 $\pm$ 6.8
August	Dry	60.2 $\pm$ 6.2	-9.2 $\pm$ 6.8
	Moderate	69.1 $\pm$ 5.7	2.1 $\pm$ 6.6
	Wet	74.8 $\pm$ 3.4	9.5 $\pm$ 9.3

**Table 3-2.** Kruskal-Wallis and Wilcoxon signed-rank test for the volumetric water content (%) and water table depth (cm) within the ‘Dry’, ‘Moderate’, and ‘Wet’ plots in July and August 2021. Note that \*, \*\*, \*\*\*, and \*\*\*\* indicate significance at 0.05, 0.01, <0.001, and <0.0001, respectively.

Month	Kruskal-Wallis VWC p-value	Kruskal-Wallis WTD p-value	Wilcoxon Pairwise Plots	Wilcoxon VWC p-value	Wilcoxon WTD p-value
July	<1.00x10 <sup>-04</sup> ****	<1.00x10 <sup>-04</sup> ****	Dry - Moderate	<1.00x10 <sup>-04</sup> ****	<1.00x10 <sup>-04</sup> ****
			Dry - Wet	<1.00x10 <sup>-04</sup> ****	<1.00x10 <sup>-04</sup> ****
			Moderate -Wet	8.40x10 <sup>-04</sup> ***	4.80x10 <sup>-02</sup> *
August	<1.00x10 <sup>-04</sup> ****	<1.00x10 <sup>-04</sup> ****	Dry - Moderate	<1.00x10 <sup>-04</sup> ****	<1.00x10 <sup>-04</sup> ****
			Dry - Wet	<1.00x10 <sup>-04</sup> ****	<1.00x10 <sup>-04</sup> ****
			Moderate -Wet	<1.00x10 <sup>-04</sup> ****	3.30x10 <sup>-04</sup> ****

### 3.2. Variations in Chlorophyll Fluorescence and Gas-Exchange Analyses

#### 3.2.1. Chlorophyll Fluorescence ( $F_v/F_m$ , $F_v'/F_m'$ , and $\phi$ PSII)

Throughout the field season, *C.aquaticus* plants displayed seasonal fluctuations in their measured dark and light-adapted chlorophyll fluorescence variables (Figure 3-2). In the ‘Dry’ experiment plots, *C.aquaticus* plants displayed an average  $F_v/F_m$  ratio of  $0.745 \pm 0.030$  in July, which subsequently decreased to  $0.726 \pm 0.033$  in August. In comparison, *C.aquaticus* within the ‘Wet’ experimental plots demonstrated comparable values in their average  $F_v/F_m$  ratio for both July and August. However, the *C.aquaticus* plants in the ‘Moderate’ experimental plots exhibited an increase in their average  $F_v/F_m$  ratio from  $0.696 \pm 0.076$  in July to  $0.714 \pm 0.040$  in August (Table 3-3). The variation observed in the dark-adapted chlorophyll fluorescence variables between months are also reflected in the light-adapted chlorophyll fluorescence variables,  $F_v'/F_m'$  and  $\phi$ PSII (Figure 3-2, 3-3). In the ‘Dry’ experimental plots, *C.aquaticus* plants demonstrated a decrease in both their average  $F_v'/F_m'$  ratio and  $\phi$ PSII from July to August (Table 3-3). In contrast, the *C.aquaticus* plants in the ‘Moderate’ experimental plots exhibited a slight increase in their average  $F_v'/F_m'$  ratio and a decrease in their  $\phi$ PSII during the same period (Table 3-3). A similar trend was also observed in the ‘Wet’ experimental plots, where *C.aquaticus* plants experienced an increase in the average  $F_v'/F_m'$  ratio and a decrease in  $\phi$ PSII from July to August (Table 3-3).

As shown in Table 3-4, the Kruskal-Wallis test was performed to assess the statistical significance of the dark and light-adapted chlorophyll fluorescence parameters between the varying moisture plots, separating them into two seasons of the study: July and August. The results indicated that the  $F_v/F_m$  ratio in July, the  $F_v'/F_m'$  ratio in both July and August, and  $\phi$ PSII in August were statistically significant, with p-values less than 0.05. To identify the specific experimental plots with statistically significant differences in July and August, the Wilcoxon

signed-rank test was used for pairwise comparison across all moisture conditions. The test revealed statistically significant differences (p-values < 0.05) in July for the  $F_v/F_m$  ratio between the 'Dry-Moderate' and 'Dry-Wet' pairwise comparison groups, while the 'Moderate-Wet' was not significant. Furthermore, all other pairwise comparisons for the  $F_v/F_m$  ratio in August were also not statistically significant (p-value > 0.05). Statistically significant differences (p-value < 0.05) were observed for the  $F_v'/F_m'$  ratio in July within the 'Dry-Moderate' pairwise group, while marginally significant differences were noted within the 'Moderate-Wet' pairwise group (p-value = 0.05). However, all pairwise comparison groups for the other moisture conditions in both July and August were not statistically significant, with p-values greater than 0.05. Moreover, statistically significant differences in  $\phi$ PSII values were detected in August for the 'Dry-Wet' and 'Moderate-Wet' pairwise groups, with p-values less than 0.05. However, all other pairwise comparison groups for  $\phi$ PSII values in both July and August did not show statistical significance, with p-values greater than 0.05.

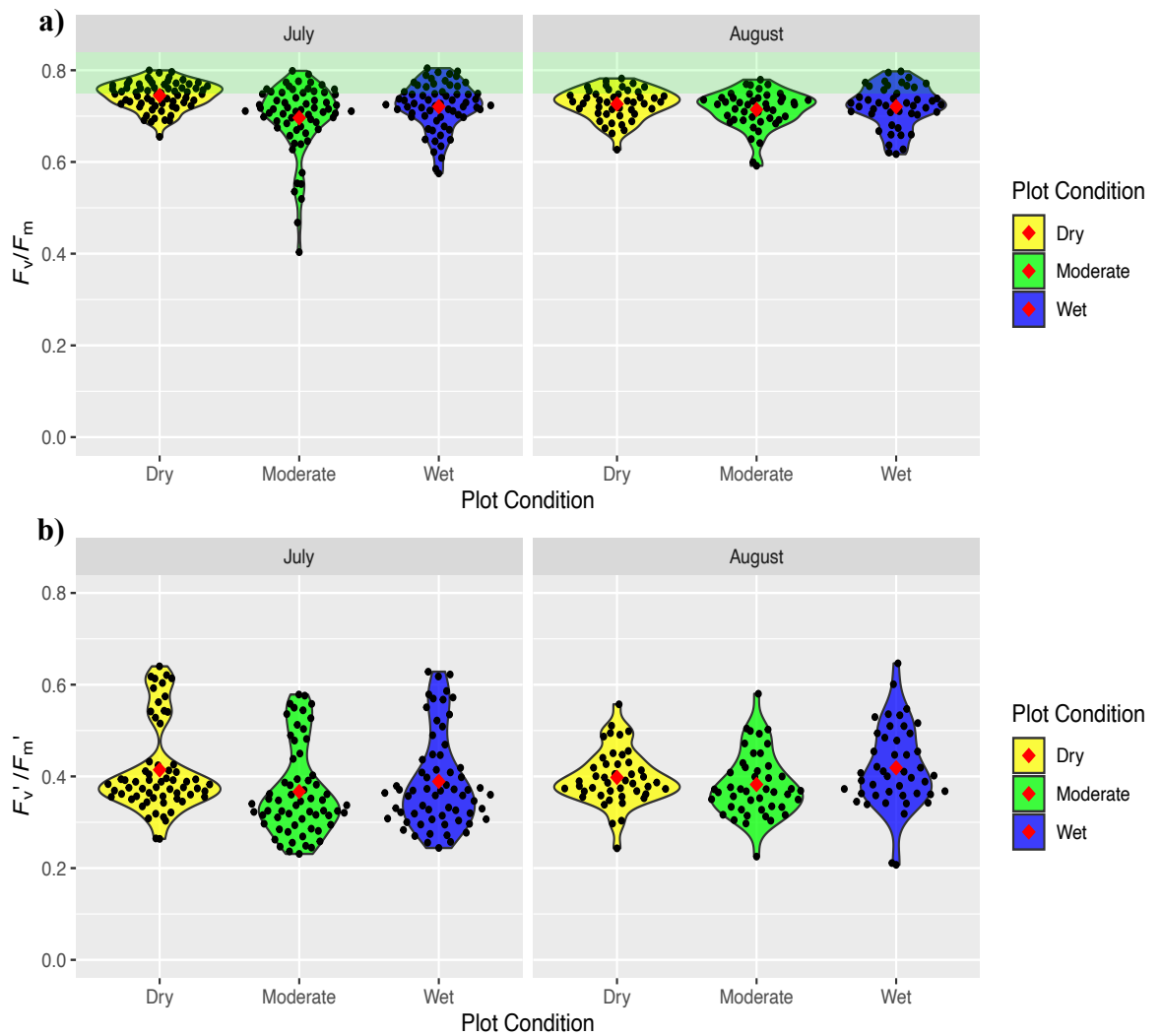


**Figure 3-2.** Violin plots in **a)** show the daily  $F_v/F_m$  ratio and in **b)**  $F_v'/F_m'$  ratio measured in July and August 2021 for the dark-adapted *Carex aquatilis* within the ‘Dry’, ‘Moderate’, and ‘Wet’ plots. Black dots indicate the daily measurements of that variable for each replicate in that specific moisture condition. The red dot represents the monthly mean of the data for that moisture condition. In plot **a)** The shaded green area signifies the approximate range (0.75+) in which plants are known to be typically healthy and unstressed

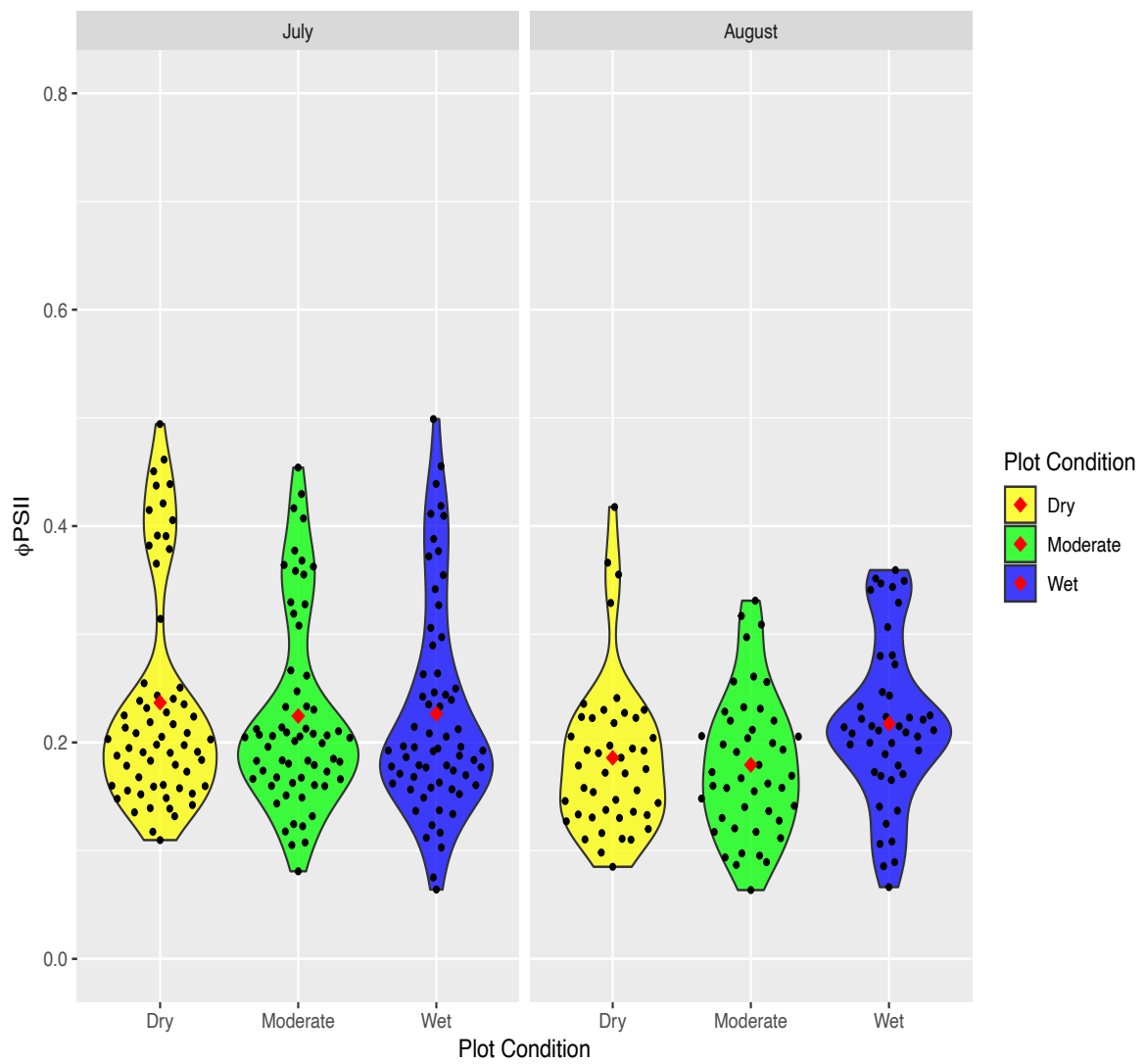


**Figure 3-3.** Violin plot demonstrating the daily  $\phi\text{PSII}$  value measured in July and August 2021 for the light-adapted *Carex aquatilis* within the ‘Dry’, ‘Moderate’, and ‘Wet’ plots. Black dots indicate the daily  $\phi\text{PSII}$  measurements for each replicate within that specific moisture condition. The red dot represents the monthly mean of the  $\phi\text{PSII}$  data for that moisture condition.

**Table 3-3.** Average stress ratio ( $F_v/F_m$ ), operating efficiency of PSII under light conditions ( $F_v'/F_m'$ ), and quantum yield of PSII under light conditions ( $\phi$ PSII) ( $\pm$  standard deviation) of *Carex aquatilis* plants in the 'Dry', 'Moderate', and 'Wet' plots within the Nikanotee fen in July and August 2021, n=109.

Month	Plot Condition	Avg $F_v/F_m \pm$ SD	Avg $F_v'/F_m' \pm$ SD	Avg $\phi$ PSII $\pm$ SD
July	Dry	0.745 $\pm$ 0.030	0.414 $\pm$ 0.097	0.237 $\pm$ 0.102
	Moderate	0.696 $\pm$ 0.076	0.367 $\pm$ 0.097	0.224 $\pm$ 0.089
	Wet	0.721 $\pm$ 0.051	0.389 $\pm$ 0.104	0.226 $\pm$ 0.098
August	Dry	0.726 $\pm$ 0.033	0.398 $\pm$ 0.059	0.186 $\pm$ 0.071
	Moderate	0.714 $\pm$ 0.040	0.382 $\pm$ 0.069	0.179 $\pm$ 0.065
	Wet	0.721 $\pm$ 0.046	0.419 $\pm$ 0.083	0.217 $\pm$ 0.076

**Table 3-4.** Kruskal-Wallis and Wilcoxon signed-rank test for the  $F_v/F_m$ ,  $F_v'/F_m'$ , and  $\phi$ PSII results within the 'Dry', 'Moderate', and 'Wet' plots in July and August 2021. Note that \*, \*\*, \*\*\*, and \*\*\*\* indicate significance at 0.05, 0.01, <0.001, and <0.0001, respectively and ns indicates not significant.

Month	KW <sup>a</sup> $F_v/F_m$ p-value	KW <sup>a</sup> $F_v'/F_m'$ p-value	KW <sup>a</sup> $\phi$ PSII p-value	Wilcoxon Pairwise Plots	Wilcoxon $F_v/F_m$ p-value	Wilcoxon $F_v'/F_m'$ p-value	Wilcoxon $\phi$ PSII p-value
July	<1.00x10 <sup>-04</sup> ****	2.46x10 <sup>-03</sup> **	8.62x10 <sup>-01</sup> ns	Dry - Moderate	<1.00x10 <sup>-04</sup> ****	1.40x10 <sup>-03</sup> **	9.00x10 <sup>-01</sup> ns
				Dry - Wet	8.30x10 <sup>-03</sup> **	7.51x10 <sup>-02</sup> ns	9.00x10 <sup>-01</sup> ns
				Moderate - Wet	7.59x10 <sup>-02</sup> ns	1.65x10 <sup>-01</sup> ns	9.00x10 <sup>-01</sup> ns
August	3.91x10 <sup>-01</sup> ns	4.26x10 <sup>-02</sup> *	1.94x10 <sup>-02</sup> *	Dry - Moderate	4.50x10 <sup>-01</sup> ns	1.45x10 <sup>-01</sup> ns	8.85x10 <sup>-01</sup> ns
				Dry - Wet	6.40x10 <sup>-01</sup> ns	3.11x10 <sup>-01</sup> ns	3.30x10 <sup>-02</sup> *
				Moderate - Wet	6.40x10 <sup>-01</sup> ns	5.10x10 <sup>-02</sup> *	3.10x10 <sup>-02</sup> *

<sup>a</sup> Kruskal – Wallis

### 3.2.2. Gas-Exchange (Transpiration, Carbon Assimilation, and Light-Response Curves)

In conjunction with the chlorophyll fluorescence variables, gas-exchange parameters such as carbon assimilation ( $a$ ), transpiration ( $E$ ), and the maximum photosynthetic capacity at saturating light levels ( $A_{max}$ ) were measured throughout the field season. Carbon assimilation and transpiration values were measured and recorded simultaneously alongside dark and light-adapted chlorophyll fluorescence results (Figure 3-4, 3-5). In July to August, the average dark transpiration and dark carbon assimilation values of *C.aquaticus* in ‘Dry’ plots increased from  $1.98 \times 10^{-5} \pm 9.57 \times 10^{-6} \text{ mm s}^{-1}$  to  $2.45 \times 10^{-5} \text{ mm s}^{-1} \pm 1.02 \times 10^{-5}$  and from  $-1.27 \pm 0.54 \text{ } \mu\text{mol m}^{-2} \text{ s}^{-1}$  to  $-0.72 \pm 0.27 \text{ } \mu\text{mol m}^{-2} \text{ s}^{-1}$ , respectively (Table 3-5). In contrast, the average light transpiration and light carbon assimilation values of *C.aquaticus* in ‘Dry’ plots decreased from  $4.25 \times 10^{-5} \text{ mm s}^{-1} \pm 1.67 \times 10^{-5}$  to  $3.40 \times 10^{-5} \pm 1.32 \times 10^{-5} \text{ mm s}^{-1}$  and from  $4.73 \pm 1.80 \text{ } \mu\text{mol m}^{-2} \text{ s}^{-1}$  to  $2.68 \pm 1.27 \text{ } \mu\text{mol m}^{-2} \text{ s}^{-1}$  during the same period (Table 3-5). Similar trends were also observed in ‘Moderate’ plots, where the average dark transpiration and dark carbon assimilation values for *C.aquaticus* increased slightly from  $2.30 \times 10^{-5} \pm 1.12 \times 10^{-5} \text{ mm s}^{-1}$  to  $2.77 \times 10^{-5} \pm 1.10 \times 10^{-5} \text{ mm s}^{-1}$  and from  $-1.28 \pm 0.53 \text{ } \mu\text{mol m}^{-2} \text{ s}^{-1}$  to  $-0.89 \pm 0.49 \text{ } \mu\text{mol m}^{-2} \text{ s}^{-1}$  in July to August, respectively (Table 3-5). However, the light average transpiration and light carbon assimilation values of *C.aquaticus* in ‘Moderate’ plots decreased from  $4.61 \times 10^{-5} \pm 1.82 \times 10^{-5} \text{ mm s}^{-1}$  to  $3.67 \times 10^{-5} \text{ mm s}^{-1} \pm 1.19 \times 10^{-5}$  and from  $4.18 \pm 1.89 \text{ } \mu\text{mol m}^{-2} \text{ s}^{-1}$  to  $2.47 \pm 1.00 \text{ } \mu\text{mol m}^{-2} \text{ s}^{-1}$  during the same period, respectively (Table 3-5). In ‘Wet’ plots, the average dark transpiration values of *C.aquaticus* decreased from  $2.39 \times 10^{-5} \pm 1.48 \times 10^{-5} \text{ mm s}^{-1}$  to  $1.90 \times 10^{-5} \pm 9.89 \times 10^{-6} \text{ mm s}^{-1}$  in July to August. Meanwhile, the average dark carbon assimilation of *C.aquaticus* in ‘Wet’ plots increased from  $-1.36 \pm 0.69 \text{ } \mu\text{mol m}^{-2} \text{ s}^{-1}$  to  $-0.76 \pm 0.37 \text{ } \mu\text{mol m}^{-2} \text{ s}^{-1}$  during the same period. In contrast, the average light transpiration and light carbon assimilation values of *C.aquaticus* in ‘Wet’ plots decreased from  $4.57 \times 10^{-5} \pm 1.85 \times$

$10^{-05} \text{ mm s}^{-1}$  to  $3.15 \times 10^{-05} \pm 1.33 \times 10^{-05} \text{ mm s}^{-1}$  and from  $4.40 \pm 2.10 \mu\text{mol m}^{-2} \text{ s}^{-1}$  to  $3.06 \pm 1.52 \mu\text{mol m}^{-2} \text{ s}^{-1}$  in July to August, respectively (Table 3-5). The maximum photosynthetic capacity at saturating light levels ( $A_{max}$ ) demonstrated similar trends to the light-adapted gas exchange variables, with values decreasing across all moisture conditions between July and August (Figure 3-6). The average  $A_{max}$  decreased for *C.aquatilis* in the 'Dry' plots from  $7.00 \pm 5.16 \mu\text{mol CO}_2 \text{ m}^{-2} \text{ s}^{-1}$  to  $2.71 \pm 1.73 \mu\text{mol CO}_2 \text{ m}^{-2} \text{ s}^{-1}$ , in the 'Moderate' plots from  $5.61 \pm 2.94 \mu\text{mol CO}_2 \text{ m}^{-2} \text{ s}^{-1}$  to  $4.90 \pm 2.39 \mu\text{mol CO}_2 \text{ m}^{-2} \text{ s}^{-1}$ , and in the 'Wet' plots from  $7.33 \pm 3.36 \mu\text{mol CO}_2 \text{ m}^{-2} \text{ s}^{-1}$  to  $6.31 \pm 4.01 \mu\text{mol CO}_2 \text{ m}^{-2} \text{ s}^{-1}$  during this period (Table 3-5).

As illustrated in Table 3-6, the Kruskal-Wallis test was utilized to determine if there were statistically significant differences in the dark/light transpiration, dark/light carbon assimilation, and  $A_{max}$  values between the varying moisture plots, separating them into two seasons of the study: July and August. The test revealed statistically significant differences (p values < 0.05) in both dark and light transpiration values for August, as well as in the  $A_{max}$  values for August (Table 3-6). The Wilcoxon signed-rank test was subsequently employed to identify statistically significant differences between the experimental moisture plots in July and August (Table 3-7). The results indicate that statistically significant differences (p-values < 0.05) in the 'Dry-Wet' and 'Moderate-Wet' plots regarding the dark transpiration values observed in August. Additionally, statistically significant differences were observed in the 'Moderate-Wet' pairwise group for the light transpiration in August. The p-values for all other pairwise comparisons of both light and dark transpiration values in July and August exceeded 0.05, indicating they were not statistically significant. The Wilcoxon signed-rank test demonstrated no statistically significant differences (p-values > 0.05) among all pairwise comparison groups for both dark and light carbon assimilation values in July and August. The Wilcoxon signed-rank test identified a statistically significant difference between the 'Dry-

Wet' pairwise group in August for the  $A_{max}$  values, with a p-value less than 0.05. However, all other pairwise comparisons for the  $A_{max}$  values in July and August did not yield statistically significant results

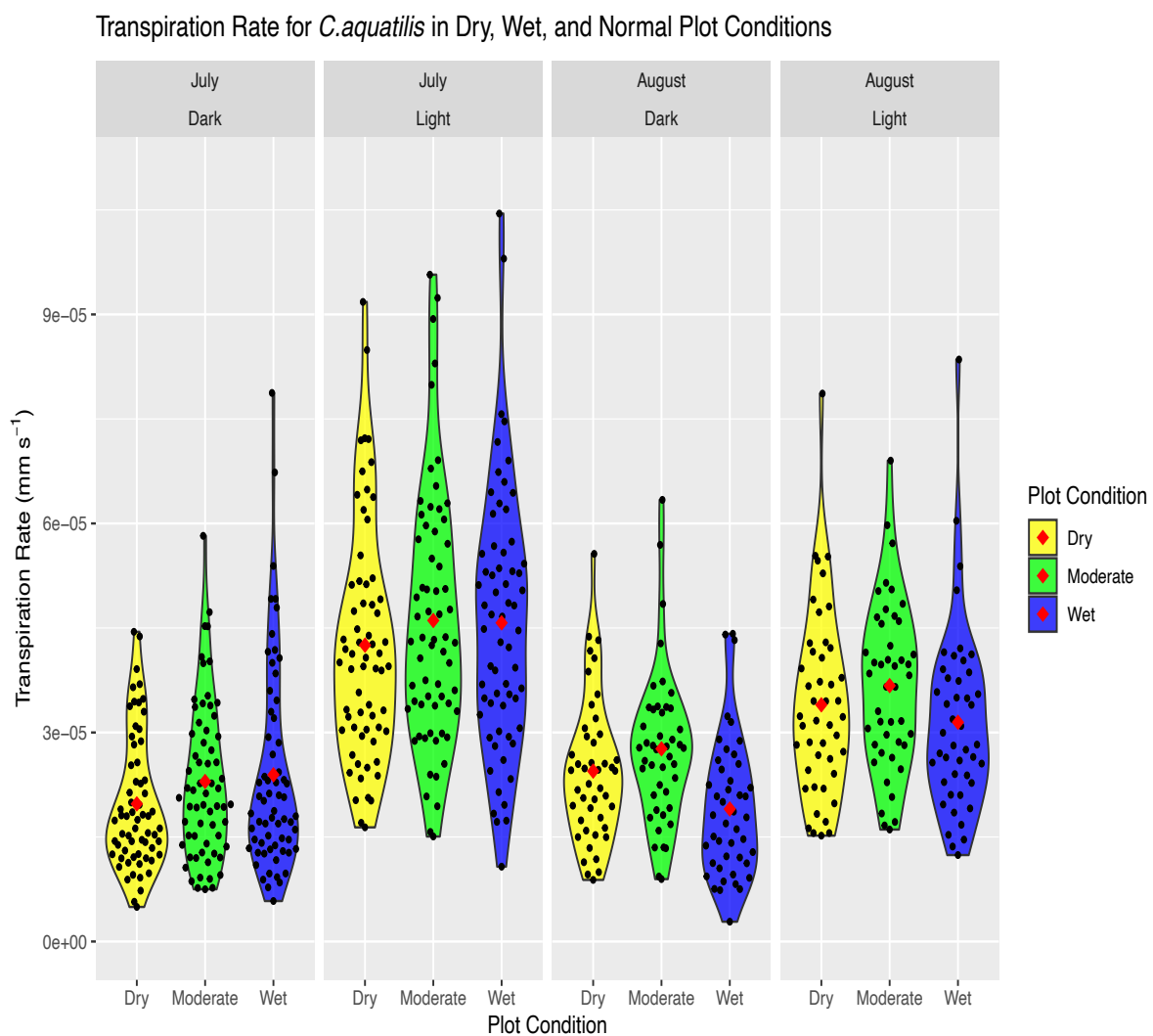


**Figure 3-4.** Violin plot demonstrating the daily dark and light transpiration rate ( $\text{mm s}^{-1}$ ) of the *Carex aquatilis* plants measured in July and August 2021 within the 'Dry', 'Moderate', and 'Wet' plots. Black dots indicate the daily transpiration rate for each replicate within that plot. The red dot represents the monthly mean of the transpiration rate data for that moisture condition.

Carbon Assimilation Rate for *C.aquatilis* in Dry, Wet, and Normal Plot Conditions

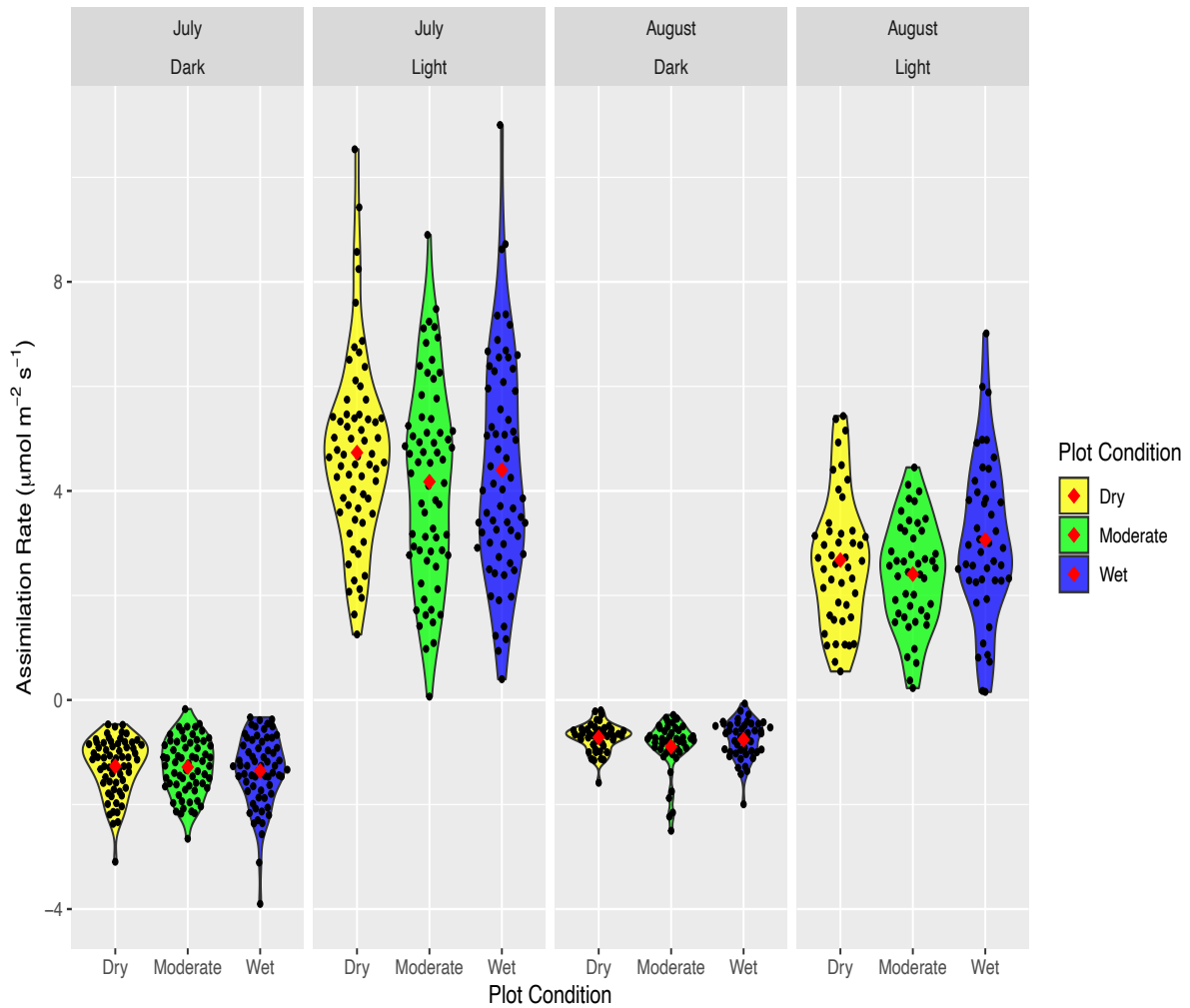


**Figure 3-5.** Violin plot displaying the daily dark and light carbon assimilation rate ( $\mu\text{mol m}^{-2} \text{s}^{-1}$ ) of the *Carex aquatilis* plants measured in July and August 2021 within the ‘Dry’, ‘Moderate’, and ‘Wet’ plots. Black dots indicate the daily assimilation rate for each replicate within that plot. The red dot represents the monthly mean of the assimilation rate data for that plot condition.

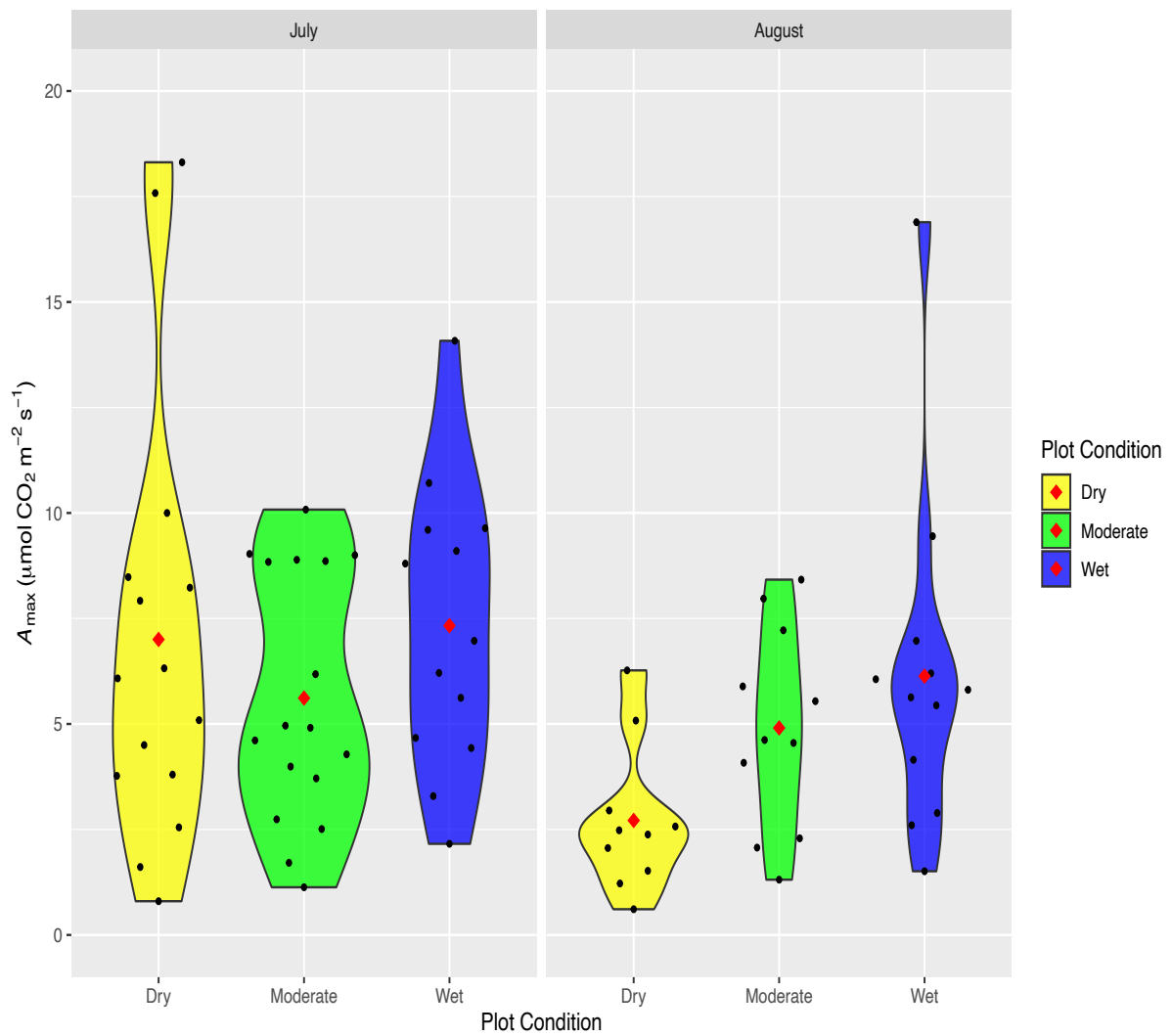


**Figure 3-6.** Violin plot illustrating the maximum photosynthetic capacity at saturating light levels ( $A_{max}$ ) ( $\mu\text{mol CO}_2 \text{ m}^{-2} \text{ s}^{-1}$ ) of the *Carex aquatilis* plants measured in July and August 2021 within the ‘Dry’, ‘Moderate’, and ‘Wet’ plots. Black dots indicate the  $A_{max}$  rate for each specific plant replicate within each plot. The red dot represents the monthly mean of the  $A_{max}$  data for that moisture condition.

**Table 3-5.** Average transpiration ( $E$ ) ( $\text{mm s}^{-1}$ ) ( $n=109$ ), carbon assimilation ( $a$ ) ( $\mu\text{mol m}^{-2} \text{s}^{-1}$ ) ( $n=109$ ), and maximum photosynthetic capacity at saturating light levels ( $A_{max}$ ) ( $\text{CO}_2 \text{ m}^{-2} \text{s}^{-1}$ ) ( $n=78$ ) ( $\pm$  standard deviation) of *Carex aquatilis* plants in the ‘Dry’, ‘Moderate’, and ‘Wet’ plots within the Nikanotee fen in July and August 2021.

Month	Plot Condition	Avg dark $E^a$ ( $\text{mm s}^{-1}$ ) $\pm$ SD	Avg light $E^a$ ( $\text{mm s}^{-1}$ ) $\pm$ SD	Avg dark $a^b$ ( $\mu\text{mol m}^{-2} \text{s}^{-1}$ ) $\pm$ SD	Avg light $a^b$ ( $\mu\text{mol m}^{-2} \text{s}^{-1}$ ) $\pm$ SD	Avg $A_{max}^c$ ( $\mu\text{mol CO}_2 \text{ m}^{-2} \text{s}^{-1}$ ) $\pm$ SD
July	Dry	$1.98 \times 10^{-5} \pm 9.57 \times 10^{-6}$	$4.25 \times 10^{-5} \pm 1.67 \times 10^{-5}$	$-1.27 \pm 0.54$	$4.73 \pm 1.80$	$7.00 \pm 5.16$
	Moderate	$2.30 \times 10^{-5} \pm 1.12 \times 10^{-5}$	$4.61 \times 10^{-5} \pm 1.82 \times 10^{-5}$	$-1.28 \pm 0.53$	$4.18 \pm 1.89$	$5.61 \pm 2.94$
	Wet	$2.39 \times 10^{-5} \pm 1.48 \times 10^{-5}$	$4.57 \times 10^{-5} \pm 1.85 \times 10^{-5}$	$-1.36 \pm 0.69$	$4.40 \pm 2.10$	$7.33 \pm 3.36$
August	Dry	$2.45 \times 10^{-5} \pm 1.02 \times 10^{-5}$	$3.40 \times 10^{-5} \pm 1.32 \times 10^{-5}$	$-0.72 \pm 0.27$	$2.68 \pm 1.27$	$2.71 \pm 1.73$
	Moderate	$2.77 \times 10^{-5} \pm 1.10 \times 10^{-5}$	$3.67 \times 10^{-5} \pm 1.19 \times 10^{-5}$	$-0.89 \pm 0.49$	$2.47 \pm 1.00$	$4.90 \pm 2.39$
	Wet	$1.90 \times 10^{-5} \pm 9.89 \times 10^{-6}$	$3.15 \times 10^{-5} \pm 1.33 \times 10^{-5}$	$-0.76 \pm 0.37$	$3.06 \pm 1.52$	$6.31 \pm 4.01$

**Table 3-6.** Kruskal-Wallis test for transpiration ( $E$ ) ( $\text{mm s}^{-1}$ ), carbon assimilation ( $a$ ) ( $\mu\text{mol m}^{-2} \text{s}^{-1}$ ), and light assimilation rate of carbon assimilation ( $A_{max}$ ) ( $\text{CO}_2 \text{ m}^{-2} \text{s}^{-1}$ ) results within the ‘Dry’, ‘Moderate’, and ‘Wet’ plots in July and August 2021. Note that \*, \*\*, \*\*\*, and \*\*\*\* indicate significance at 0.05, 0.01, <0.001, and <0.0001, respectively and ns indicates not significant.

Month	Kruskal - Wallis dark $E$ p-value	Kruskal - Wallis light $E$ p-value	Kruskal - Wallis dark $a$ p-value	Kruskal - Wallis light $a$ p-value	Kruskal - Wallis $A_{max}$ p-value
July	$2.15 \times 10^{-01} \text{ns}$	$4.30 \times 10^{-01} \text{ns}$	$7.07 \times 10^{-01} \text{ns}$	$3.89 \times 10^{-01} \text{ns}$	$3.93 \times 10^{-01} \text{ns}$
August	$2.26 \times 10^{-04} \text{***}$	$5.66 \times 10^{-02} *$	$3.02 \times 10^{-01} \text{ns}$	$1.97 \times 10^{-01} \text{ns}$	$2.82 \times 10^{-02} *$

**Table 3-7.** Wilcoxon signed-rank test for transpiration ( $E$ ) ( $\text{mm s}^{-1}$ ), carbon assimilation ( $a$ ) ( $\mu\text{mol m}^{-2} \text{s}^{-1}$ ), and light assimilation rate of carbon assimilation ( $A_{\text{max}}$ ) ( $\text{CO}_2 \text{ m}^{-2}\text{s}^{-1}$ ) results within the ‘Dry’, ‘Moderate’, and ‘Wet’ plots in July and August 2021. Note that \*, \*\*, \*\*\*, and \*\*\*\* indicate significance at 0.05, 0.01, <0.001, and <0.0001, respectively and ns indicates not significant.

Month	Wilcoxon Pairwise Plots	Wilcoxon dark $E$ p-value	Wilcoxon light $E$ p-value	Wilcoxon dark $a$ p-value	Wilcoxon light $a$ p-value	Wilcoxon $A_{\text{max}}$ p-value
July	Dry - Moderate	$2.70 \times 10^{-01\text{ns}}$	$4.10 \times 10^{-01\text{ns}}$	$7.90 \times 10^{-01 \text{ns}}$	$4.10 \times 10^{-01\text{ns}}$	$7.90 \times 10^{-01\text{ns}}$
	Dry - Wet	$2.70 \times 10^{-01\text{ns}}$	$4.10 \times 10^{-01\text{ns}}$	$7.90 \times 10^{-01 \text{ns}}$	$4.10 \times 10^{-01\text{ns}}$	$7.00 \times 10^{-01\text{ns}}$
	Moderate - Wet	$8.10 \times 10^{-01\text{ns}}$	$9.50 \times 10^{-01\text{ns}}$	$7.90 \times 10^{-01 \text{ns}}$	$7.50 \times 10^{-01\text{ns}}$	$4.30 \times 10^{-01\text{ns}}$
August	Dry - Moderate	$9.99 \times 10^{-02\text{ns}}$	$2.60 \times 10^{-01\text{ns}}$	$3.00 \times 10^{-01 \text{ns}}$	$6.50 \times 10^{-01\text{ns}}$	$9.20 \times 10^{-02\text{ns}}$
	Dry - Wet	$1.37 \times 10^{-02**}$	$2.60 \times 10^{-01\text{ns}}$	$9.50 \times 10^{-01 \text{ns}}$	$3.60 \times 10^{-01\text{ns}}$	$2.70 \times 10^{-02*}$
	Moderate - Wet	$1.60 \times 10^{-04****}$	$4.70 \times 10^{-02*}$	$4.80 \times 10^{-01 \text{ns}}$	$2.20 \times 10^{-01\text{ns}}$	$5.25 \times 10^{-01\text{ns}}$

### 3.3. Variations in Salinity of Belowground, Aboveground, and Litter Biomass

At the end of the field season in August, samples of aboveground, belowground, and litter biomass were gathered from *C.aquaticus* plants across all moisture plots and examined for their sodium concentration levels. Belowground biomass samples were separated into the three soil depths: 0-10 cm, 10-30 cm, and 30-50 (Figure 3-7). The average sodium concentration in the 0-10 cm soil depth varied among the *C.aquaticus* plants across the 'Dry', 'Moderate', and 'Wet' plots, increasing from  $1381.5 \pm 430.6$  mg/kg to  $1667.6 \pm 747.8$  mg/kg, and  $1998.0 \pm 1038.5$  mg/kg, respectively (Table 3-8). Conversely, within the 10-30 cm soil depth, the average sodium concentrations were comparable for *C.aquaticus* plants in the 'Moderate' and 'Wet' plots, measuring at  $2012.0 \pm 720.3$  mg/kg and  $2280.0 \pm 619.6$  mg/kg, respectively. However, *C.aquaticus* plants in the 'Dry' plots exhibited the highest concentration at  $3103.0 \pm 1568.6$  mg/kg within the 10-30 cm depth. At 30-50 cm soil depth, *C.aquaticus* plants displayed similar average sodium concentrations across the 'Dry', 'Moderate', and 'Wet' plots, measuring at  $2989.2 \pm 1912.9$  mg/kg,  $2773.0 \pm 1518.7$  mg/kg, and  $2802.3 \pm 1472.2$  mg/kg, respectively. As observed in Figure 3-8, the average sodium concentration in the aboveground biomass of *C.aquaticus* plants were  $1155.2 \pm 680.6$  mg/kg,  $2184.2 \pm 272.0$  mg/kg, and  $3017.2 \pm 889.6$  mg/kg for the 'Dry', 'Moderate', and 'Wet' plots, respectively. The sodium concentrations in the litter biomass of *C.aquaticus* were relatively steady, measuring at  $1834.7 \pm 772.3$  mg/kg,  $1934.4 \pm 779.5$  mg/kg, and  $2091.6 \pm 665.1$  mg/kg for the 'Dry', 'Moderate', and 'Wet' plots, respectively (Table 3-9).

The Kruskal-Wallis test was employed to evaluate whether there were any statistically significant differences in the sodium concentrations among the belowground, aboveground, and litter biomass samples of *C.aquaticus* between the varying moisture plots, separating them into the three collected depths: 0-10, 10-30, and 30-50 cm. As indicated in Table 3-10, the

Kruskal-Wallis test revealed no statistically significant differences (p-value > 0.05) in sodium concentration among the belowground biomass samples for any of the three soil depths collected across all moisture conditions. Consequently, the Wilcoxon signed-rank test also revealed no statistically significant differences (p-value > 0.05) among all moisture pairwise comparison groups at the three soil depths. Similarly, in Table 3-11, the Kruskal-Wallis test showed no statistically significant difference across all moisture conditions in the litter biomass samples of *C.aquatilis*, and the Wilcoxon signed-rank test yield the same outcome, with no statistically significant difference observed across all pairwise comparison groups. However, as seen in Table 3-11, the Kruskal-Wallis test revealed statistically significant differences in the aboveground biomass of *C.aquatilis* across the varying moisture levels, with a p-value less than 0.05. The Wilcoxon signed-rank test revealed statistically significant differences in the ‘Dry-Moderate’ and ‘Dry-Wet’ pairwise groups, with p-values less than 0.05, whereas the ‘Moderate-Wet’ group was not statistically significant, with a p-value greater than 0.05.

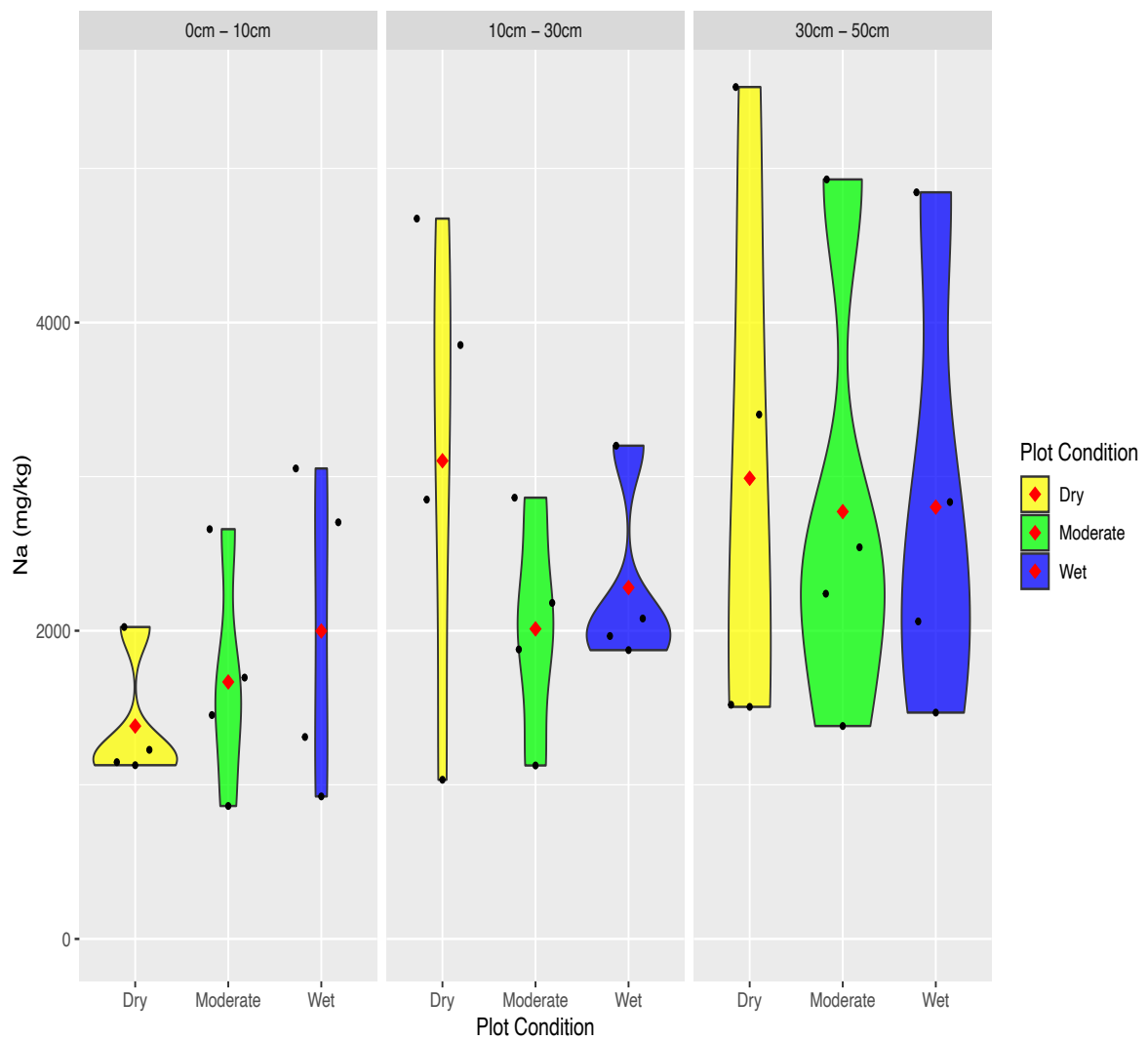


**Figure 3-7.** Violin plot illustrating the belowground biomass sodium concentration (mg/kg) of the *Carex aquatilis* plants in 0-10 cm, 10-30 cm, and 30-50 cm soil levels within the ‘Dry’, ‘Moderate’, and ‘Wet’ plots. Black dots indicate the sodium concentration for each specific replicate within each plot. The red dot represents the mean of the sodium concentration data for that moisture condition.

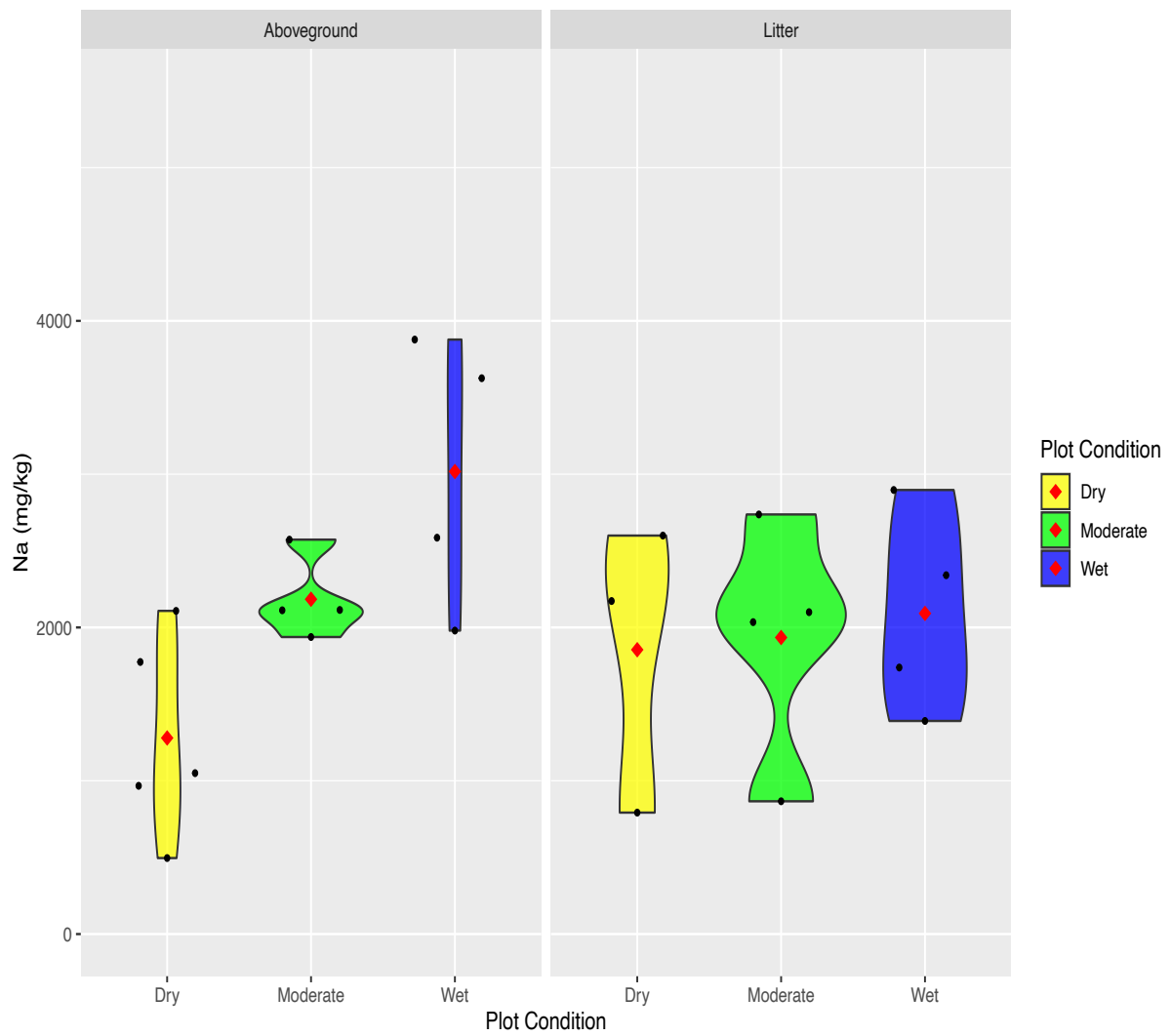


Figure 3-8. Violin plot illustrating the aboveground and litter biomass sodium concentration (mg/kg) of the *Carex aquatilis* plants within the 'Dry', 'Moderate', and 'Wet' plots. Black dots indicate the sodium concentration for each specific replicate within each plot. The red dot represents the mean of the sodium concentration data for that moisture condition.

**Table 3-8.** Average ( $\pm$  standard deviation) belowground biomass sodium concentrations of the *Carex aquatilis* plants at depths of 0-10cm (n =12), 10-30cm (n =12), and 30-50cm (n =12) within the ‘Dry’, ‘Moderate’, and ‘Wet’ plot conditions in the Nikanotee fen, August 2021.

Plot Condition	Soil Level (cm)	Avg Below Na <sup>+</sup> [ ] (mg/kg) $\pm$ SD
Dry	0-10	1381.5 $\pm$ 430.6
	10-30	3103.0 $\pm$ 1568.6
	30-50	2989.2 $\pm$ 1912.9
total average		<b>2491.2 <math>\pm</math> 1547.1</b>
Moderate	0-10	1667.6 $\pm$ 747.8
	10-30	2012.0 $\pm$ 720.3
	30-50	2773.0 $\pm$ 1518.7
total average		<b>2169.1 <math>\pm</math> 1184.5</b>
Wet	0-10	1998.0 $\pm$ 1038.5
	10-30	2280.0 $\pm$ 619.6
	30-50	2802.3 $\pm$ 1472.2
total average		<b>2360.1 <math>\pm</math> 1054.1</b>

**Table 3-9.** Average ( $\pm$  standard deviation) aboveground (n=12) and litter (n=12) biomass sodium concentrations of the *Carex aquatilis* plants within the ‘Dry’, ‘Moderate’, and ‘Wet’ plot conditions in the Nikanotee fen, August 2021.

Plot Condition	Avg Above Na <sup>+</sup> [ ] (mg/kg) $\pm$ SD	Avg Litter Na <sup>+</sup> [ ] (mg/kg) $\pm$ SD
Dry	1155.2 $\pm$ 680.6	1834.7 $\pm$ 772.3
Moderate	2184.2 $\pm$ 272.0	1934.4 $\pm$ 779.5
Wet	3017.2 $\pm$ 889.6	2091.6 $\pm$ 665.1

**Table 3-10.** Kruskal-Wallis and Wilcoxon signed-rank test for the belowground biomass sodium concentration in the *Carex aquatilis* plants at depths of 0-10 cm, 10-30 cm, and 30-50 cm under the ‘Dry’, ‘Moderate’, and ‘Wet’ plot conditions in the Nikanotee fen, August 2021. Note that \*, \*\*, \*\*\*, and \*\*\*\* indicate significance at 0.05, 0.01, <0.001, and <0.0001, respectively and ns indicates not significant.

Soil Level (cm)	Kruskal-Wallis p-value	Wilcoxon Pairwise Plots	Wilcoxon Below p-value
0-10	6.18E-01 <sup>ns</sup>	Dry - Moderate	6.90x10 <sup>-01ns</sup>
		Dry - Wet	6.90x10 <sup>-01ns</sup>
		Moderate -Wet	6.90x10 <sup>-01ns</sup>
10-30	5.84E-01 <sup>ns</sup>	Dry - Moderate	7.30x10 <sup>-01ns</sup>
		Dry - Wet	7.30x10 <sup>-01ns</sup>
		Moderate -Wet	8.90x10 <sup>-01ns</sup>
30-50	9.44E-01 <sup>ns</sup>	Dry - Moderate	1.00 <sup>ns</sup>
		Dry - Wet	1.00 <sup>ns</sup>
		Moderate -Wet	1.00 <sup>ns</sup>

**Table 3-11.** Kruskal-Wallis and Wilcoxon signed-rank test for the aboveground and litter biomass sodium concentration in the *Carex aquatilis* plants under the ‘Dry’, ‘Moderate’, and ‘Wet’ plot conditions in the Nikanotee fen, August 2021. Note that \*, \*\*, \*\*\*, and \*\*\*\* indicate significance at 0.05, 0.01, <0.001, and <0.0001, respectively and ns indicates not significant.

Kruskal-Wallis Above p-value	Kruskal-Wallis Litter p-value	Wilcoxon Pairwise Plots	Wilcoxon Above p-value	Wilcoxon Litter p-value
2.06x10 <sup>-02*</sup>	9.31x10 <sup>-01ns</sup>	Dry - Moderate	4.80x10 <sup>-02*</sup>	1.00 <sup>ns</sup>
		Dry - Wet	4.80x10 <sup>-02*</sup>	1.00 <sup>ns</sup>
		Moderate -Wet	2.00x10 <sup>-01ns</sup>	1.00 <sup>ns</sup>

## Chapter 4. Discussion

### 4.1. The Role of Edaphic Conditions on *Carex aquatilis* Productivity Parameters

#### 4.1.1. Seasonal Variability in Edaphic Conditions

As demonstrated through the results of this study, the functionality of *C.aquatilis* was examined under varying moisture conditions. As demonstrated in Figure 3-1b, the average volumetric water content (VWC) remained consistent within each moisture condition and fluctuated minimally through the study. However, the average water table depth (WTD) increased from the months of July to August (Figure 3-1a). The rise in WTD is attributed to the increased rainfall frequency and decreased temperatures during these months. Despite the variable edaphic conditions observed throughout the study, the VWC and WTD remained within acceptable ranges to support the growth and functionality of *C.aquatilis*. While specific values for ideal VWC and WTD conducive to optimal growth of *C.aquatilis* are not well-defined in current literature, they have been observed in areas where the WTD ranges from -80 cm below to 37 cm above the base of the plant (Kopochork et al. 2012). However, *C.aquatilis* is predominantly found in areas where the WTD ranges from -20 cm to 20 cm above the plant base, indicating a preference for wetter sights, although it can exist in drier environments (Kopochork et al. 2012). Additionally, previous research on the distribution of peatland vegetation in natural fens has shown that *C.aquatilis* dominates wet fens where the average depth to water table is around 10.9 cm (Graham et al., 2016). While *C.aquatilis* often form lawns in naturally wet fens, it can also be found in drier fens, though with less coverage, where the average depth to water table is approximately 12.9 cm (Graham et al., 2016).

Notably, the field season in early July commenced with record-breaking temperatures, minimal precipitation, and elevated PAR levels (Figure 2-3). Although the VWC and WTD remained relatively stable across all moisture conditions in July and August, one replicate within the 'Wet' plots experienced drying during this period of extreme temperature (30°C+).

This led to a decline in the daily average VWC in July, as shown in Figure 3-1b. Eventually, the specific replicate gradually recovered as the frequency of rainfall events increased during the season. The hydrological regime in peatlands is a critical ecological factor that profoundly influences the structural and functional aspects of the vegetation community (Yao et al., 2021). Changes in the water regime, including fluctuations in water table depth and soil moisture content, can significantly impact the composition and distribution of wetland plant species, as well as the availability of essential elements crucial for their functionality (Hájek et al., 2013; Yao et al., 2021). Rising water table levels and extended periods of waterlogging can disrupt the soil redox potential of the vegetation community, leading to reduced concentrations of specific elements and an increase in the production of harmful phytotoxins (Mainiero & Kazda, 2005). Conversely, reductions in water table levels and prolonged exposure to drought conditions can impact the carbon balance within peatlands (Potvin et al., 2015). Decreased water levels can accelerate peat oxidation and modify the net primary production rate of the vegetation community, resulting in the ecosystem shifting from a carbon sink to a carbon source (Potvin et al., 2015). Peatland vegetation varies significantly among species in terms of their physiology and responses to alterations in hydrology and water stress (Potvin et al., 2015). Under waterlogged conditions, *Carex* species develop aerenchyma tissue, facilitating the transport of oxygen into their roots and enabling the development of deep rooting zones (Loreti & Perata, 2020; Potvin et al., 2015). Additionally, under high water levels and anaerobic stress, *Carex* species may employ techniques such as radical oxygen loss (ROL) to ensure the release of oxygen through the aerenchyma tissue to the rhizosphere (Lai et al., 2012). During prolonged drought conditions, wetland *Carex* species may employ morphological adaptations, such as biomass allocation, by reducing their leaf mass to decrease stomatal size and respiration, while simultaneously increasing their root to shoot ratio to access resources from deeper layers in the soil (Gao et al., 2015; Jiang et al., 2023; Zhang et al., 2020). Throughout the study, the

experimental plots fluctuated both temporally and seasonally, but the ‘Wet’ plots remained wet, while the ‘Dry’ plots stayed dry. The ‘Moderate’ plots experienced the most variation between wet and dry conditions. However, no prolonged waterlogged or drought periods occurred during the field season that affected the structural or functional characteristics of *C.aquaticus*.

#### 4.1.2. Chlorophyll Fluorescence

Numerous prior studies have explored the morphological and physiological adaptations utilized by various *Carex* species within wetlands globally, demonstrating their capacity to thrive amidst fluctuating hydrological regimes (Mainiero & Kazda, 2005; Zhang et al., 2020). However, within the AOSR, few studies have explored adaptations and mechanisms employed by *C.aquaticus* in reclaimed wetlands and post-mined sites. Despite the experimental plots maintaining optimal moisture levels for the growth and survival of *C.aquaticus*, fluctuations in abiotic factors could provide valuable insights into the species’ rapid response and adaptive mechanisms during stressful conditions. Notably, Vitt et al. (2011) demonstrated that *C.aquaticus* in re-established well sites of the Peace River region of Alberta experienced rapid proliferation and superior growth performance in wetter areas compared to drier areas from 2007 to 2009 (Vitt et al., 2011). Although the range and variability of WTD in this study is narrower (Figure 3-1a) compared to Vitt et al. (2011), it was still anticipated that *C.aquaticus* would demonstrate higher productivity and less stress in the ‘Wet’ plots within the Nikanotee Fen compared to other moisture conditions. However, upon examining the dark and light-adapted chlorophyll fluorescence results from the experiment, those expected outcomes were not observed. Specifically, when assessing the maximum quantum efficiency of photosystem II (PSII) ( $F_v/F_m$ ), also known as the stress ratio, the *C.aquaticus* plants in the ‘Dry’, ‘Wet’ and ‘Moderate’ moisture conditions exhibited similar average values in July and August ranging from 0.69 to 0.74 (Table 3-3). While a portion of the daily dark-adapted  $F_v/F_m$  measurements

for *C.aquaticus* across the soil moisture conditions yielded values of 0.75 or higher, the majority of the data fell below this range (Figure 3-2a). According to numerous previous studies on chlorophyll fluorescence, both theoretical and empirical evidence suggests that the average  $F_v/F_m$  ratio for healthy, unstressed plants is approximately  $\sim 0.83$  and higher (Baker, 2008; Maxwell & Johnson, 2000; Murchie & Lawson, 2013). However, the portable photosynthesis system (LI-6800) used for chlorophyll fluorescence measurements in this experiment, specifies that the variable to maximal value for the  $F_v/F_m$  ratio ranges between 0.75 to 0.85 (LI-COR, 2022). This range is contingent upon factors such as species, leaf health and age, and pre-conditioning treatment (LI-COR, 2022). The  $F_v/F_m$  ratio serves as an indicator of the intrinsic functionality of PSII, providing insight into the photosynthetic performance of plants by determining the maximum quantum efficiency at which PSII absorbs light and utilizes it for the reduction of electron acceptor,  $Q_A$ , thereby facilitating photochemical energy conversion (Baker, 2008). Higher  $F_v/F_m$  ratios often indicate that a larger portion of absorbed light is effectively used for photosynthesis, suggesting high potential productivity and efficient photosynthetic performance (Baker, 2008). Variations in the  $F_v/F_m$  ratio primarily reflect changes in the photochemical efficiency of PSII, often due to the onset of photoinhibition caused by stress (Baker, 2008). Consistent declines in the  $F_v/F_m$  ratio over time may indicate that the non-photochemical quenching processes are insufficient in dissipating excess light energy as heat, leading to irreversible damage to the photosynthetic apparatus (Maxwell & Johnson, 2000). The average stress ratio values of *C.aquaticus* in each moisture condition were slightly below the ideal range as described in previous literature, with few plants measuring at 0.75 and above, and none exceeding 0.8. The  $F_v/F_m$  ratios observed in this study are similar to those reported by Mollard et al. (2012), where *C.aquaticus* in the industrial wetlands of Fort McMurray, Alberta had  $F_v/F_m$  ratios of 0.75. Notably in this study, the  $F_v/F_m$  ratios showed statistically significant differences ( $p$ -value  $< 0.05$ ) between the 'Dry' plots and both the 'Wet'

and ‘Moderate’ plots in July (Table 3-4). Additionally, in July, it is observed that few  $F_v/F_m$  ratios fell below 0.6 in both the ‘Wet’ and ‘Moderate’ plots (Figure 3-2a). These statistically significant findings and anomalies observed in July are interpreted to be the result of the higher temperatures and PAR values observed at the beginning of the field season, which created drier biophysical surface conditions (Figure 2-3). The *C.aquatilis* in ‘Dry’ plot were less affected by the heat stress, possibly because of the shade provided by the small trees growing within those sections of the Nikanotee fen, unlike the ‘Wet’ and ‘Moderate’ plots, which were fully exposed to the sun. Shading in the ‘Dry’ plots might have deterred photoinhibition in the *C.aquatilis* plants and enabled the incoming light energy to be utilized for effective photochemical quenching activities like photosynthesis, thereby explaining the stability observed in their  $F_v/F_m$  ratio measurements (Maxwell & Johnson, 2000; Murchie & Lawson, 2013). Conversely, *C.aquatilis* in the ‘Wet’ and ‘Moderate’ plots demonstrated decreases in their  $F_v/F_m$  ratio, suggesting a shift in the efficacy of their photochemical processes and their ability to absorb light. As a result of heat stress, photoinhibition is often noted with decreases in  $F_v/F_m$  ratio (Maxwell & Johnson, 2000; Murchie & Lawson, 2013). Furthermore, substantially lower  $F_v/F_m$  ratios were observed in the *C.aquatilis* within the ‘Moderate’ plots compared to those in the ‘Dry’ and ‘Wet’ plots. The area with the ‘Moderate’ plots within the Nikanotee fen experience consistently fluctuating water and moisture levels throughout the season, potentially hindering the development of morphological and physiological adaptations formed under extended periods of waterlogged and drought conditions, unlike the *C.aquatilis* in the ‘Dry’ and ‘Wet’ plots. Consequently, the absence of these adaptations could potentially have led to lower  $F_v/F_m$  ratio values, as stressors such as elevated heat and drought may reduce the efficiency of photochemical processes, prioritizing the utilization of light energy for survival and protection rather than photosynthesis (Maxwell & Johnson, 2000; Zhang et al., 2020). As the season progressed and the heat wave subsided, the  $F_v/F_m$  ratios for *C.aquatilis* in the ‘Wet’ and

'Moderate' plots returned to Moderate levels, with statistically insignificant differences among the plots in August. Analyzing the overall  $F_v/F_m$  ratio results from all experimental plots suggests that *C.aquaticus* remained relatively unstressed and maintained efficient levels of light absorption for photochemistry, despite varying soil moisture and water table depths. Although the threshold for moisture stress was not reached in this study, *C.aquaticus* maintained stable functionality and productivity in the Nikanotee Fen throughout the growing season. Instead, sudden environmental changes, such as heat stress, appeared to more significantly disrupt their light absorption ability and overall functionality than variations in moisture conditions. However, it is worth noting that the  $F_v/F_m$  ratio for *C.aquaticus* across all moisture conditions remained in the lower range typically observed in healthy, unstressed plants. Although this study does not explain the cause for lower  $F_v/F_m$  ratios, it highlights the interplay between various environmental factors and *C.aquaticus* photochemistry in a reclaimed wetland, suggesting a need for further investigation.

The light-adapted chlorophyll fluorescence variables,  $F_v'/F_m'$  and  $\phi$ PSII, were also analysed under varying moisture conditions. The  $F_v'/F_m'$  ratio serves as the counterpart to the stress ratio, offering insights into the maximum efficiency of PSII under actinic light conditions (Baker, 2008). It reflects the ability of PSII to use absorbed light for photochemistry when all reaction centres are open and electron acceptor  $Q_A$  is oxidized, indicating the capacity of PSII to drive photochemical processes effectively (Baker, 2008). This parameter can provide an indication on the influence of non-photochemical quenching processes on changes in PSII efficiency within the light (Baker, 2008). Although precise ranges for the  $F_v'/F_m'$  ratio are not explicitly specified in current literature, values should fall below those of the  $F_v/F_m$  ratio (Baker, 2008; Maxwell & Johnson, 2000; Murchie & Lawson, 2013). Similar to the  $F_v/F_m$  ratio, higher  $F_v'/F_m'$  values indicate a greater proportion of absorbed light used for photochemistry, suggesting efficient light utilization and higher potential productivity (Baker, 2008).

Conversely, lower values may indicate reduced efficiency in light absorption, potentially due to the presence of stressor (Baker, 2008). The  $F_v'/F_m'$  ratio is ideally lower than the stress ratio due to the competition between non-photochemical and photochemical quenching processes within the leaf for light energy in plants adapted to actinic light conditions, leading to a reduction in the value (LI-COR, 2022). The  $F_v'/F_m'$  ratios measured for the *C.aquatilis* in the 'Dry', 'Wet', and 'Moderate' plots demonstrated overall lower averages in July and August in comparison to the  $F_v/F_m$  ratio (Figure 3-2b). Kruskal-Wallis tests revealed statistically significant results in both July and August (p-value < 0.05). Further examination using the Wilcoxon signed-rank test revealed significant results (p-value < 0.05) between the 'Dry' and 'Moderate' plots in July and marginal differences (p = 0.05) between the 'Moderate' and 'Wet' plots in August (Table 3-4). The statistically significant differences observed in the  $F_v'/F_m'$  ratio between the 'Dry' and 'Moderate' plots in July may also have been attributed to the heatwave experienced at the beginning of the field season. As previously discussed, *C.aquatilis* plants in the 'Moderate' plot were fully exposed to the sunlight within the fen, whereas those in the 'Dry' plots experienced shading from small trees. Declines in the  $F_v'/F_m'$  ratio observed in the 'Moderate' plots may suggest an increase in the non-photochemical processes or the onset of photoinhibition within the *C.aquatilis* plants (Maxwell & Johnson, 2000; Murchie & Lawson, 2013). This decrease may indicate a shift in the use of light energy towards protective mechanisms in the plant or the formation of reactive oxygen species, rather than its utilization for photochemical processes (Maxwell & Johnson, 2000; Zhang et al., 2020). In contrast to the 'Dry' plots and 'Wet' plots, *C.aquatilis* within the 'Moderate' plots may lack physiological adaptations necessary to cope with heat stress and arid conditions. The marginally significant differences (p-value = 0.05) in August between the *C.aquatilis* within the 'Moderate' and 'Wet' plots may not necessarily signify issues with the efficiency of PSII in light conditions. The distribution of the data between both plots appear similar with no significant outliers (Figure

3-3) and there are no apparent environmental or moisture factors potentially affecting productivity of *C.aquatilis* within either plot. While it was anticipated that these results observed in both  $F_v/F_m$  and  $F_v'/F_m'$  ratios would be reflected in the  $\phi$ PSII measurements, this was not the case.  $\phi$ PSII offers insights into the actual operational efficiency of PSII across different light and environmental settings, providing the proportion of absorbed light utilized for photochemical electron transport in PSII (Baker, 2008; Maxwell & Johnson, 2000; Murchie & Lawson, 2013). Unlike both  $F_v/F_m$  and  $F_v'/F_m'$  ratios,  $\phi$ PSII directly measures real-time efficiency of PSII in performing photochemistry by accounting for both photochemical and non-photochemical energy processes (Baker, 2008). While non-photochemical quenching processes does not directly affect the  $F_v/F_m$  ratio, it does directly influence both  $F_v'/F_m'$  and  $\phi$ PSII by reducing these values (Baker, 2008; Maxwell & Johnson, 2000; Murchie & Lawson, 2013). Like  $F_v'/F_m'$ , consistently low  $\phi$ PSII values caused by prolonged exposure to extreme light intensity can saturate non-photochemical quenching processes, reducing the capacity of PSII to utilize light energy and potentially causing damage to the photosynthetic apparatus (Baker, 2008). Subsequently, ideal ranges for  $\phi$ PSII values vary widely among species and age groups, and specific values for *C.aquatilis* are not established within current literature. However, like the other chlorophyll fluorescence parameters, high  $\phi$ PSII values indicate that a greater proportion of absorbed light is being utilized for photosynthesis, suggesting a high potential productivity (Baker, 2008). Upon analysing the overall averages of  $\phi$ PSII values for *C.aquatilis*, a decline is observed from July to August (Figure 3-3) across all moisture conditions. Furthermore, statistically significant differences (p-value < 0.05) were noted in August for the pairwise comparison groups between the 'Dry' and 'Wet' plots, as well as between the 'Moderate' and 'Wet' plots. During the heatwave in July, reductions were observed in both  $F_v/F_m$  and  $F_v'/F_m'$  ratios, yet the  $\phi$ PSII values for *C.aquatilis* across all moisture conditions remained stable during that time. These results may suggest that, despite

a decrease in the efficiency of PSII to utilize absorbed light photochemistry under both dark and actinic conditions, *C.aquaticus* was able to maintain a consistent proportion of absorbed light used for photochemistry in real-time (Baker, 2008; Maxwell & Johnson, 2000; Murchie & Lawson, 2013). The stability of  $\phi$ PSII under heat stress suggests that *C.aquaticus* may be adapting to stress by effectively managing light energy, despite demonstrating reduced maximum efficiency of PSII (Baker, 2008; Demmig-Adams & Adams, 2006; Maxwell & Johnson, 2000). Although this study cannot determine the exact reason for the stability of  $\phi$ PSII in July, the results highlight the overall effective functionality and productivity of *C.aquaticus* in Nikanotee Fen throughout the field season despite sudden environmental stressors. They also suggest that *C.aquaticus* may employ mechanisms to respond to environmental stress while maintaining effective light utilization for photochemical processes. In August, *C.aquaticus* in the 'Wet' plots exhibited slightly higher  $\phi$ PSII values compared to *C.aquaticus* in both the 'Dry' and 'Moderate' plots. These statistically significant differences observed between the 'Dry' and 'Wet' plots, as well as between the 'Moderate' and 'Wet' plots, do not correspond with any notable environmental stressors that would account for these variations. Additionally, the consistency of  $\phi$ PSII values across all moisture conditions in July, with measurements remaining insignificant (p-value > 0.05), suggests that varying moisture levels do not significantly affect  $\phi$ PSII. Therefore, the observed differences in August might not be directly related to changes in soil moisture. It's worth noting that *C.aquaticus* measured within 'Moderate' plots demonstrated lower average  $\phi$ PSII values in both July and August. These lower  $\phi$ PSII averages within in the 'Moderate' plot may have a similar explanation for the decreased values observed in  $F_v/F_m$  and  $F_v'/F_m'$  ratios during the heatwave. This could be attributed to the potential absence of physiological and morphological adaptations required to respond effectively to abrupt abiotic stressors, resulting in an overall reduction in their photosynthetic capacity. The phenomena of hormesis observed in numerous plant species

might elucidate why *C.aquaticus* plants thrive in both the waterlogged conditions of the ‘Wet’ plots and the drought conditions of the ‘Dry’ plots. Hormesis refers to the response whereby low doses of abiotic stressors over extended periods stimulate physiological mechanisms aimed at enhancing plant growth and mitigating stress (Jalal et al., 2021). On the contrary, exposure to abrupt high doses of abiotic stressors often results in irreversible and adverse effects on the health and functioning of plants (Jalal et al., 2021). This phenomenon has been observed in various *Carex* species, where abiotic stressors like increasing water depth stimulate productivity and survival by triggering physiological and morphological adaptations (Sorrell et al., 2012). However, the exact reasoning for why the *C.aquaticus* demonstrated statistically significant  $\phi$ PSII values in August cannot be deduced from the data available. This may suggest other factors other than the measured environmental conditions in this study may be influencing  $\phi$ PSII.

#### **4.1.3. Transpiration, Carbon Assimilation, and Light Response Curves**

The transpiration rate, a crucial gas-exchange parameter, offers valuable insights into the functioning of plant stomatal complexes (Nilson & Assmann, 2007). The capacity and rate at which plants transpire under different abiotic stressors are crucial, as reducing water loss and facilitating nutrient transport are vital for survival (Nilson & Assmann, 2007). Monitoring transpiration rate is essential for comprehending plant productivity and responses to changing environmental conditions, including fluctuations in soil moisture. The average transpiration rates measured in the dark-adapted *C.aquaticus* were similar between July and August across the different moisture conditions (Figure 3-4). However, the light-adapted *C.aquaticus* showed a decrease in the average transpiration rates from July and August across all moisture conditions, with light-adapted transpiration rates higher than dark-adapted rates (Table 3-5). Higher transpiration rates in the light-adapted *C.aquaticus* are expected, as plants transpire more rapidly in the light than darkness, since light stimulates the opening of the

stomata (Nilson & Assmann, 2007). After performing the Wilcoxon signed-rank test, both the dark and light-adapted transpiration rates of *C.aquaticus* plants in August exhibited statistically significant differences ( $p$ -value  $< 0.05$ ) between the 'Dry' to 'Wet' plots and the 'Moderate' to 'Wet' plots. Transpiration rates of *C.aquaticus* within the 'Dry' and 'Moderate' plots were higher than those in the 'Wet' plots, as plants under waterlogged conditions often demonstrate a decrease in stomatal conductance (Ashraf, 2012). Waterlogged conditions and water stress typically cause the stomata to close, resulting in reduced rates of transpiration and photosynthesis (Ashraf, 2012). The lower transpiration rates observed in the *C.aquaticus* plants in the 'Wet' plots could be attributed to the waterlogged conditions, exacerbated by an increase in the frequency of rain events in August. However, as previously discussed, the chlorophyll fluorescence parameters ( $F_v/F_m$ ,  $F_v'/F_m'$ ,  $\phi$ PSII) did not indicate reduced levels of functionality, as the *C.aquaticus* in the 'Wet' plots exhibited higher average values at times than those in the 'Dry' and 'Moderate' plots. The specific cause behind these statistically significant results, whether it be moisture levels or another environmental factor, cannot be determined conclusively based on this experiment. It is noteworthy that previous research conducted by Mollard et al. (2012) examined the transpiration rate of *C.aquaticus* in the industrial wetlands of Fort McMurray. Mollard et al. (2012) measured gas exchange parameters (transpiration and net CO<sub>2</sub> exchange) simultaneously with chlorophyll fluorescence parameters using an infrared gas analyzer during the first two weeks of June 2011. Although moisture levels were not considered, *C.aquaticus* in industrial wetlands exhibited an average transpiration rate of  $7.67 \times 10^{-5} \text{ mm s}^{-1}$  (Mollard et al., 2012). The average transpiration rates for the light-adapted *C.aquaticus* in all moisture conditions within this experiment were lower than this, averaging between  $3.15 \times 10^{-5}$  and  $4.61 \times 10^{-5} \text{ mm s}^{-1}$ . Although the precise reasons for the lower range of transpiration rate of *C.aquaticus* in the Nikanotee fen are not clearly evident from this experiment, factors such as moisture levels and differences between years the two studies were

conducted may play a role. Similarly, the carbon assimilation rate was measured in both dark and light-adapted *C.aquatilis* across each experimental moisture condition. Carbon assimilation is an intricate and complex process vital for the survival of plants due to its impact on their energy-related processes, such as photosynthesis (Irving, 2015). The rate of carbon assimilation offers valuable insights into a plant's photosynthetic capacity, measuring its ability to convert carbon from the atmosphere into organic compounds (Zhou et al., 2021). Various environmental factors and stressors can impact plant physiology, influencing their capacity to absorb carbon and, consequently, their overall productivity (Loreto & Centritto, 2008). When examining the dark-adapted *C.aquatilis* average carbon assimilation rates, a decrease in respiration was observed from July to August across all moisture plots, as the values become less negative. Additionally, the carbon assimilation rate for the light-adapted *C.aquatilis* showed a decrease during the same period. The seasonal changes observed in carbon assimilation rates in both dark and light-adapted *C.aquatilis* plants may be a physiological response to changing environmental conditions in July and August. This study does not conclusively identify the specific factors directly impacting the carbon assimilation rate, but fluctuations in moisture levels and temperatures could be contributors to these results. The literature extensively documents the effects of water stress, as plants often decrease their stomatal conductance in both waterlogged and drought conditions (Loreto & Centritto, 2008). This reduction limits the entry of carbon dioxide into leaves, thereby diminishing carbon assimilation and metabolism (Loreto & Centritto, 2008). Additionally, Strack et al. (2014) investigated methane (CH<sub>4</sub>) and CO<sub>2</sub> fluxes within the restored sections of a peatland in the WBP. Their study accounted for fluctuating water table levels and included a range of peatland vegetation, from mosses to vascular species such as *C.aquatilis* (Strack et al., 2014). They determined that graminoids made up a significant portion of plant cover in the peatland and were positively correlated with water table levels, serving as a key factor influencing the

relationship between CO<sub>2</sub> exchange and water table fluctuations (Strack et al., 2014). Furthermore, they observed that wetter restored plots had higher graminoid and vascular plant cover, resulting in greater net CO<sub>2</sub> uptake compared to the drier restored plots (Strack et al., 2014). Notably, their work highlights the importance of managing water levels in restored peatlands, as wetter sites can act as CO<sub>2</sub> sinks but may also become significant CH<sub>4</sub> sources if excessively wet (Strack et al., 2014). In contrast, they found that drier sites tend to act as CO<sub>2</sub> sources, and that shallow water table levels contribute to increased CH<sub>4</sub> emissions (Strack et al., 2014). Although their study focused on a variety of vegetation rather than just solely sedges, similar patterns in carbon assimilation and uptake might be expected in this study, particularly in August as precipitation levels increased over the season. However, this was not observed, and rather, decreases in carbon assimilation were seen across all water table and soil moisture levels. Most research on how sedges respond to changes in water levels vary drastically between species, as the *Carex* genus thrive in both high and low water table levels (Zhong et al., 2020). Despite the observed trends in the average rates of dark and light-adapted carbon assimilation, further statistical analysis revealed no statistically significant differences across all moisture conditions either July or August. The lack of statistically significant results suggests that moisture may not be a significant factor affecting carbon assimilation rates in this study, or that the moisture ranges tested were insufficient to impact the carbon assimilation rate. Although statistically significant decreases were observed in some chlorophyll fluorescence parameters for *C.aquatilis* in the ‘Moderate’ plots in August, similar trends were expected to be observed in the carbon assimilation rate. As previously mentioned, *C.aquatilis* in the ‘Wet’ plots demonstrated lower average transpiration rates than those in the ‘Moderate’ and ‘Dry plots that was not reflected in their carbon assimilation rate. This reduction in transpiration in the ‘Wet’ plots may be attributed to high water levels, potentially leading to stomatal closure without adversely affecting carbon uptake and photosynthetic activity.

Furthermore, the long adventitious roots of *C.aquaticus*, which can extend 50 cm to 1 meter below the surface, enable it to penetrate deeply into the soil, allowing access to water amid fluctuating water table depths and soil moisture levels (Popović et al., 2022). This adaptability may account the seasonally driven changes in carbon assimilation observed in this study. In Mollard et al. (2012) assessment of *C.aquaticus* in industrial wetlands of Fort McMurray, the net carbon dioxide exchange rate was recorded at  $3.19 \mu\text{mol m}^{-2} \text{s}^{-1}$  (Mollard et al., 2012). Although the net carbon dioxide exchange and carbon assimilation rate signify different aspects of carbon metabolism, the carbon assimilation values of *C.aquaticus* within this experiment ranged from  $3.06$  to  $4.73 \mu\text{mol m}^{-2} \text{s}^{-1}$ , demonstrating consistency. This observation is noteworthy, considering the recorded transpiration rate of *C.aquaticus* in this experiment were lower than those reported by Mollard et al. (2012). While the reasons for this discrepancy cannot be concluded from this study, *C.aquaticus* carbon assimilation remains largely unaffected by varying soil moisture conditions, maintaining efficient levels of light utilization for photochemical reactions.

To gain a deeper understanding of the effects of varying moisture levels on the productivity of *C.aquaticus*, light response curves were conducted to measure the maximum photosynthetic rate,  $A_{max}$ . Various photosynthetic curves are calculated in response to factors such as fluctuating carbon dioxide, temperature, and light to obtain intrinsic information about species-specific characteristics and quantify vital photochemical parameters (Reavis et al., 2023). Specifically, light response curves are used to characterize the photosynthetic response of a plant once equilibrated to fluctuating light levels and intensities (Reavis et al., 2023). Light response curves conducted within the field often diverge from those conducted in laboratory settings due to the inclusion of environmental factors typically overlooked in controlled conditions (Reavis et al., 2023). Although  $A_{max}$  values vary depending on the

environment and growing conditions of a plant, those grown at higher light intensities generally exhibit a greater  $A_{max}$  compared to plants grown at lower light intensities (Reavis et al., 2023). The average  $A_{max}$  values of *C.aquaticus* across all moisture conditions were compared between July and August, with a noted decrease between the two months. This decrease was expected due to the decline in PAR values over the season, leading to less available light (Reavis et al., 2023). Further statistical analysis revealed significant differences between *C.aquaticus* in the 'Dry' and 'Wet' plots, with plants in the 'Dry' plots showing much lower average  $A_{max}$  values compared to those in the 'Wet' plots. The difference in moisture levels between the *C.aquaticus* in the 'Dry' and 'Wet' plots may contribute to the lower values observed in the 'Dry' plots. Plants subjected to extended periods of drought and dry conditions typically exhibit lower  $A_{max}$  values, suggesting a diminished photosynthetic capacity (Jassey & Signarbieux, 2019). However, no statistically significant differences in the  $A_{max}$  values were observed in the other pairwise comparisons conducted in July, indicating that moisture levels may not be the primary factor influencing the  $A_{max}$  values. As previously noted, *C.aquaticus* in the 'Dry' plots were situated in sections of the Nikanotee fen shaded by small trees. The availability of environmental light is crucial in the photosynthetic process of plants, and reductions or shading result in decreased  $A_{max}$  values (Chen et al., 2014). The shading and reduced PAR observed in the 'Dry' plots in August likely resulted in a decrease in the light energy available for photosynthesis. Consequently, this can lead to a reduction in the rate at which plants perform this process, as indicated by the lower  $A_{max}$  value. The direct cause of the reduction in the  $A_{max}$  values observed in this experiment remains unclear. Nonetheless, these findings suggest that factors beyond moisture levels may influence the photosynthetic process. For instance, light availability could play a significant role and may be overlooked when selecting the placing of key species like *C.aquaticus* for reclamation projects in wetlands within the AOSR.

## 4.2. Impacts of Salinity on the Overall Productivity of *Carex aquatilis*

### 4.2.1. Litter, Aboveground, and Belowground Biomass Sodium Concentration

Increasing salinity levels and their potential effects on reclaimed wetlands are significant considerations in constructing these landscapes within the AOSR. Particularly in the Nikanotee Fen, which relies on sodium-rich groundwater from the upland aquifer formed from tailing sands (Kessel et al., 2018; Yang et al., 2022). The possibility of a shift towards more salt-tolerant species and the sustained productivity of the environment are key concerns in this regard (Kessel et al., 2018; Yang et al., 2022). Measuring sodium concentrations in both aboveground and belowground biomass of *C.aquatilis* across the experimental moisture plots offers insights into the salt content within vital plant organs (Glaeser et al., 2021; Vitt et al., 2020). Precisely quantifying sodium levels within salt-tolerant species such as *C.aquatilis* enhances the understanding of sodium storage mechanisms and their responses to elevating salinity levels (Glaeser et al., 2021; Vitt et al., 2020). Vitt et al. (2020) established the salinity threshold for *C.aquatilis*, observing a distinct decline in performance and eventual mortality between 1079 and 2354 mg L<sup>-1</sup> (Vitt et al., 2020). Measuring sodium concentrations within this experiment in both aboveground and belowground biomass of *C.aquatilis* enables the assessment whether these levels in the Nikanotee Fen are approaching the threshold established by Vitt et al. (2020). Yang et al. (2022) analysed the spatiotemporal patterns of salinity within the Nikanotee Fen in 2019, demonstrating that sodium concentrations varied across different depths and at the surface. Measurements of sodium concentrations at depths of 30 cm and 50 cm exhibited greater consistency compared to those taken at the surface suggesting that these depths were less influenced by factors such as precipitation and evapotranspiration (Yang et al., 2022). Furthermore, Yang et al. (2022) illustrated that salinity concentrations within the upper 35 cm of the fen in 2019 had escalated five-fold to 292 mg L<sup>-1</sup> from levels recorded at the initial construction of the Nikanotee fen in 2013. Additionally, Yang et al. (2022)

demonstrated that the sodium concentration increases from lower depths to the surface of the fen (Yang et al., 2022). The findings presented by Yang et al. (2022) and the threshold established by Vitt et al. (2020) were taken into consideration during the analysis of the litter, aboveground, and belowground biomass concentrations collected from the various moisture condition plots in this experiment. When examining the belowground biomass data gathered at depths of 0 – 10 cm, 10 – 30 cm, and 30 – 50 cm for *C.aquaticus* in the ‘Dry’, ‘Wet’ and ‘Moderate’ plots, an overall increase in average sodium concentration was observed within increasing depth (Table 3-8). However, contrary to this trend, *C.aquaticus* in the ‘Moderate’ plots exhibited higher average sodium concentrations in the 10 – 30 cm depth compared to the 30 – 50 cm depth. Although the results were not statistically significant ( $p$ -value  $> 0.05$ ) across all depths collected in the varying moisture conditions, they were intriguing given the demonstration of Yang et al. (2022) increased salinity in the upper depths of the fen. It was anticipated that the initial depth collected, 0 – 10 cm of the belowground biomass, would exhibit a higher salt concentration than the lower depths to reflect the salt gradient in the surrounding water of the fen. This could imply potential mechanisms utilized by *C.aquaticus* to limit the entry of sodium into the roots through different salt exclusion methods (Munns, 2002; Munns & Tester, 2008). Possibly, *C.aquaticus* may employ selective ion uptake, favouring the absorption of ions such as potassium over sodium from the surrounding upper soil depths, thereby hindering sodium entry (Munns, 2002; Munns & Tester, 2008). Furthermore, the absence of statistical significance across all depths, coupled with the consistent total averages in the sodium concentrations across all varying moisture plots, suggests that moisture conditions may not significantly influence the concentration of sodium in the belowground biomass of *C.aquaticus*. When examining the average litter sodium concentrations collected, no statistically significant differences were observed among the Dry’, ‘Wet’, and ‘Moderate’ plots, with similar averages recorded. Given that the experimental moisture plots were

distributed across different areas of the fen, it was expected that the litter within 'Dry' plots might have higher sodium concentrations compared to the areas with the 'Moderate' and 'Wet' plots. This was anticipated because areas experiencing drier conditions and drought tend to accumulate salt at the surface of the soil due to reduced water availability, however, this was not observed within this experiment (Alvarez Rogel et al., 2000). Furthermore, the increase in rain events in August, could have potentially decreased sodium concentrations within the litter samples in the 'Dry' plots, resulting in similar sodium concentrations to those observed in the 'Wet' and 'Moderate' plots. If the litter sampling had been consistently conducted throughout the season, including earlier in July amidst the intense heat and sparse rainfall, a clearer trend in sodium concentration across the plots with varying moisture conditions could have been identified. Notably, when examining the average sodium concentrations in the aboveground biomass of *C.aquatilis* across different moisture conditions, it was observed that the 'Wet' plots exhibited the highest average, followed by 'Moderate' plots, and 'Dry' plots. Wilcoxon signed-rank tests revealed statistically significant results ( $p$ -value  $< 0.05$ ) between pairwise groups of *C.aquatilis* in both the 'Dry' to 'Wet' plots and the 'Dry' to 'Moderate' plots. These findings are noteworthy because, unlike the results observed in the belowground biomass, they may suggest that the availability of moisture influences the uptake of sodium in the aboveground biomass of *C.aquatilis*. Vitt et al. (2020) determined that the sodium concentration detected in the belowground biomass of *C.aquatilis* exceeded that of the aboveground biomass in the laboratory. While soil moisture levels were not considered in their study, they suggested that *C.aquatilis* may employ a salt exclusion mechanism at the roots to prevent the accumulation of sodium in the leaves to toxic concentrations (Vitt et al., 2020). However, in this field study, it was observed that only the *C.aquatilis* plants in the 'Dry' plots exhibited a higher total sodium concentration in their belowground biomass compared to their aboveground biomass. Conversely, the *C.aquatilis* in the 'Moderate' plots showed similar sodium concentrations in

both their belowground and aboveground biomass. Meanwhile, those in the ‘Wet’ plots displayed a significantly higher sodium concentration in their aboveground biomass compared to their belowground biomass, almost 261% greater. These findings demonstrate that although *C.aquaticus* in the ‘Dry’ plots may potentially employ the salt exclusion method described in Vitt et al. (2020), the mechanisms utilized in the field may vary and depend on the available moisture conditions. The increased sodium concentration in the aboveground biomass of *C.aquaticus* in the ‘Wet’ plots compared to their belowground biomass may be attributed to the abundant moisture, which facilitates the transportation of salts through the transpiration stream (Munns, 2002; Munns & Tester, 2008). Over time, this process leads to the accumulation of salt within the leaves as water evaporates, resulting in higher concentrations of sodium (Munns, 2002; Munns & Tester, 2008). Eventually, the accumulation of sodium in the older leaves reach levels that can be lethal to the cells, leading to cell death and subsequent shedding of the leaves (Munns, 2002; Munns & Tester, 2008). The mechanism of sodium accumulation occurs among plants exposed to high levels of salt uptake, leading to the development of specific salt-related adaptations over time and the emergence of salt-tolerant species (Munns, 2002; Munns & Tester, 2008). The presence of this mechanisms observed in the *C.aquaticus* throughout this experiment suggests a potential adaptation employed by the species to withstand elevated saline conditions in the Nikanotee Fen (Munns, 2002; Munns & Tester, 2008). Additionally, the decreased transpiration rate observed in the ‘Wet’ plots may have been attributed to elevated sodium concentrations in the aboveground biomass. Increased salt accumulation within the leaves can hinder water absorption from the soil by elevating the osmotic potential (Munns, 2002; Munns & Tester, 2008). Consequently, this prompts stomatal closure to mitigate water loss, resulting in a reduced transpiration rate (Munns, 2002; Munns & Tester, 2008). Notably, Mollard et al. (2012) performed a chemical analysis comparing the leaves of *C.aquaticus* grown in industrial oil sands versus those from natural wetland, and determined

that the leaves of *C.aquaticus* in industrial oil sands exhibited higher sodium concentrations compared to those in natural wetlands, alongside indications of elevated potassium/sodium ratio. These results confirm elevated levels of salinity within the leaves as demonstrated throughout this study (Mollard et al., 2012). While moisture levels were not considered, the elevated potassium/sodium ratios suggests potential salt exclusion mechanisms employed by the species, favouring potassium ions over sodium (Mollard et al., 2012). This prevents sodium from accumulating to harmful levels, which otherwise lead to reduced photosynthetic capacity or plant death (Mollard et al., 2012). Although potassium/sodium ratios were not investigated in this experiment, it is possible over time, *C.aquaticus* may have adjusted its mechanisms in response to increasing salinity levels in the AOSR. Additionally, changes in environmental factors such as climate and moisture availability within these sites may influence which mechanisms are utilized. The insights gained from this study and previous research are significant as they shed light on the diverse adaptation that *C.aquaticus* may employ in reclaimed wetlands, with their effectiveness dependent on the environmental factors existing in these sites.

## Chapter 5. Conclusion

This study assessed how fluctuating soil moisture levels affect various fluorescence and gas productivity parameters of *C.aquaticus*, while also evaluating its overall functional capacity in a developing saline environment. Analysis of both productivity parameters and biomass sodium concentrations suggests that the overall productivity of *C.aquaticus* is not solely impacted by moisture levels but was instead influenced by various environmental factors that interact with moisture. Specifically, this study demonstrated that varying moisture conditions and fluctuating water table levels had no significant impact on the functionality of *C.aquaticus*, as shown by the measurement and analysis of key chlorophyll parameters, including  $F_v/F_m$ ,  $F_v'/F_m'$ , and  $\phi$ PSII. However, unlike moisture conditions, the heatwave in July caused statistically significant decreases in the  $F_v/F_m$  and  $F_v'/F_m'$  ratios in both the 'Wet' and 'Moderate' plots compared to those in the 'Dry' plots. Specifically, the *C.aquaticus* in the 'Moderate' plots demonstrated notably lower  $F_v/F_m$  and  $F_v'/F_m'$  ratios, indicating higher stress levels compared to the 'Dry' and 'Wet' plots. Although the exact cause of the decreases in these parameters in the 'Moderate' plots cannot be determined from this study, it is possible these plots experienced consistent fluctuations in water table and moisture levels within the fen. As a result of these fluctuations, *C.aquaticus* in the 'Moderate' plots may not have developed physiological adaptations that arise from prolonged exposure to waterlogged and drought conditions, thus affecting their ability to respond to stress and maintain productivity compared to plants grown in the 'Dry' and 'Wet' plots. Furthermore, the potential shading of small trees from the sun in the 'Dry' plots might have mitigated the negative effects of the intense heat, resulting in higher  $F_v/F_m$  and  $F_v'/F_m'$  ratios. After the the heat wave,  $F_v/F_m$  and  $F_v'/F_m'$  ratios in all moisture plots returned to optimal levels, although they remained on the lower end, reflecting the complex interactions of environmental factors and conditions at specific times during the field season. Additionally, while it was expected the  $\phi$ PSII values of *C.aquaticus* in

the 'Wet' and 'Moderate' plots would demonstrate a similar decrease as previously observed in July, statistically significant results were only observed in August. The lack of decreases in the  $\phi\text{PSII}$  values indicate that while the efficiency of photosystem II might be disrupted by short-term stress event such as heat, the actual ability of photosystem II to convert light energy for photochemical energy remains unaffected. Stable values of  $\phi\text{PSII}$  may indicate the compensation of other non-photochemical quenching processes that are not accounted for in  $F_v/F_m$  ratio, thereby protecting the plants under stress (Baker, 2008; Maxwell & Johnson, 2000). The reasons behind the statistically significant results observed in August, particularly the higher  $\phi\text{PSII}$  values of *C.aquaticus* in the 'Wet' plots compared to the 'Dry' and 'Moderate' plots, cannot be conclusively determined from this experiment alone. Other environmental factors present in the Nikanotee Fen may have contributed to these findings. However, the elevated  $\phi\text{PSII}$  values of *C.aquaticus* in the 'Wet' plots, despite the increased sodium concentrations in the aboveground biomass, further demonstrates its capacity to maintain productivity and functionality in a reclaimed wetland.

Similarly, gas exchange parameters measured throughout the study revealed intriguing findings that are significant when evaluating the effects of soil moisture on the productivity of *C.aquaticus*. While the carbon assimilation rates across all moisture conditions did not show statistically significant differences, the transpiration rate in *C.aquaticus* within the 'Wet' plots was lower compared to the 'Dry' and 'Moderate' plots. Although lower transpiration rates in the 'Wet' plots may be attributed to excess moisture, the exact cause cannot be determined from this study. However, this did not impair the ability of *C.aquaticus* to function effectively in the 'Wet' plots throughout the season. The light response curves conducted in this study further revealed statistically significant decreases in the  $A_{max}$  rates within the *C.aquaticus* in the 'Dry' plots compared to the 'Wet' plots. Like the previous discussed variables, these results cannot be attributed solely to the varying moisture level. Instead, the presence of shading from

the small trees within the ‘Dry’ plots may have been the primary factor, as shading reduces the availability light energy, leading to decreased  $A_{max}$  rates. The findings from the gas-exchange parameters underscore the interconnectedness of environmental factors in dynamic ecosystems like Nikanotee fen, emphasizing the importance of considering all factors when assessing the overall productivity of a species.

The relationship between key environmental factors and the productivity of *C.aquatilis* is further illustrated by sodium concentrations found in the litter, as well as in both the aboveground and belowground biomass samples. While moisture levels and water table depth had no significant impact on the sodium concentrations in the both litter and belowground biomass of *C.aquatilis*, they did affect the aboveground biomass, with plants in the ‘Wet’ plots exhibiting higher sodium levels compared to the ‘Dry’ and ‘Moderate’ plots. Despite the elevated sodium concentrations, *C.aquatilis* in the ‘Wet’ plots maintained relatively stable  $F_v/F_m$  and  $F_v'/F_m'$  ratio, as previously noted. Combining the results from the chlorophyll fluorescence parameters and sodium analysis suggests that *C.aquatilis* in the ‘Wet’ plots can sustain efficient levels of photochemistry despite high moisture levels and salt exposure. Notably, as previously mentioned, the ‘Wet’ plots only exhibited decreases in  $F_v/F_m$  and  $F_v'/F_m'$  ratios during the heatwave, suggesting the combined effects of elevated salt levels and heat may have intensified the stress on the plants. In the ‘Dry’ plots, *C.aquatilis* demonstrated lower sodium concentrations in the aboveground biomass. These results, in conjunction with the chlorophyll analysis, suggest that the plants in the ‘Dry’ plots were unaffected by the heatwave, likely due to the absence of salt stress and the protective influence of the surrounding shaded plants, as previously discussed.

After analysing the comprehensive results gathered during this study, it cannot be conclusively stated that varying soil moisture does not influence chlorophyll fluorescence and gas-exchange productivity parameters. Instead, it may be suggested that soil moisture and

water depth might not be the predominant factor affecting *C.aquaticus*. While soil moisture and water table depth levels remained within optimal ranges for the growth and functioning of *C.aquaticus*, no significant declines were observed in any measured productivity parameters over the course of the season. However, this study demonstrated that environmental factors, such as soil moisture, may influence productivity when exposed to sudden stressors in constantly changing and fluctuating environments like reclaimed fens. The reduced values in the dark and light-adapted fluorescence parameters observed in *C.aquaticus* grown in the ‘Moderate’ plots suggest a less efficient recovery compared to its counterparts in the ‘Dry’ and ‘Wet’ plots when exposed to heat stress. This implies that when constructing the vegetation communities of reclaimed wetlands, focusing on introducing *C.aquaticus* in areas with consistent moisture levels and water table depths may be crucial for it to develop the necessary adaptations required to remain productive amidst fluctuating environmental factors and stressors. Additionally, this field study reaffirms the conclusions drawn from various laboratory experiments, highlighting *C.aquaticus* as a resilient and advantageous species for incorporation into vegetation communities with challenging environments like the reclaimed wetlands in the AOSR. Moreover, amidst concerns regarding elevated salinity in reclaimed sites, this study illustrates *C.aquaticus*’s ability to maintain productivity and adapt salt tolerance mechanisms according to its surrounding environment and moisture conditions. Additional research is needed to investigate the intricate relationship between major environmental factors and the productivity of *C.aquaticus*, as well as to understand the role of salt tolerance mechanisms in the overall functionality of the species. As global warming progresses, increased temperatures and reduced rainfall may affect the resilience of *C.aquaticus* in the AOSR, potentially altering its functionality and physiological characteristics. Moreover, elevated salinity levels, coupled with rising temperature, could influence how *C.aquaticus*

responds to salt and other abiotic stressors, potentially hindering the complete reclamation of these vital landscapes.

## References

- Alvarez Rogel, J., Alcaraz Ariza, F., & Ortiz Silla, R. (2000). Soil salinity and moisture gradients and plant zonation in Mediterranean salt marshes of Southeast Spain. *Wetlands*, 20(2), 357–372. [https://doi.org/10.1672/0277-5212\(2000\)020\[0357:ssamga\]2.0.co;2](https://doi.org/10.1672/0277-5212(2000)020[0357:ssamga]2.0.co;2)
- Baker, N. R. (2008). Chlorophyll fluorescence: A probe of photosynthesis in vivo. In *Annual Review of Plant Biology* (Vol. 59). <https://doi.org/10.1146/annurev.arplant.59.032607.092759>
- Biagi, K. M., Oswald, C. J., Nicholls, E. M., & Carey, S. K. (2019). Increases in salinity following a shift in hydrologic regime in a constructed wetland watershed in a post-mining oil sands landscape. *Science of the Total Environment*, 653, 1445–1457. <https://doi.org/10.1016/j.scitotenv.2018.10.341>
- Borkenhagen, A. K., & Cooper, D. J. (2019a). Establishing vegetation on a constructed fen in a post-mined landscape in Alberta's oil sands region: A four-year evaluation after species introduction. *Ecological Engineering*, 130(August 2018), 11–22. <https://doi.org/10.1016/j.ecoleng.2019.01.023>
- Borkenhagen, A. K., & Cooper, D. J. (2019b). Establishing vegetation on a constructed fen in a post-mined landscape in Alberta's oil sands region: A four-year evaluation after species introduction. *Ecological Engineering*, 130(January), 11–22. <https://doi.org/10.1016/j.ecoleng.2019.01.023>
- Chasmer, L., Hopkinson, C., Montgomery, J., & Petrone, R. (2016). A Physically Based Terrain Morphology and Vegetation Structural Classification for Wetlands of the Boreal Plains, Alberta, Canada. *Canadian Journal of Remote Sensing*, 42(5), 521–540. <https://doi.org/10.1080/07038992.2016.1196583>

- Chen, A., Lichstein, J. W., Osnas, J. L. D., & Pacala, S. W. (2014). Species-independent down-regulation of leaf photosynthesis and respiration in response to shading: Evidence from six temperate tree species. *PLoS ONE*, *9*(4).  
<https://doi.org/10.1371/journal.pone.0091798>
- Demmig-Adams, B., & Adams, W. W. (2006). Photoprotection in an ecological context: The remarkable complexity of thermal energy dissipation. *New Phytologist*, *172*(1), 11–21.  
<https://doi.org/10.1111/j.1469-8137.2006.01835.x>
- Elmes, M. C., & Price, J. S. (2019). Hydrologic function of a moderate-rich fen watershed in the Athabasca Oil Sands Region of the Western Boreal Plain, northern Alberta. *Journal of Hydrology*, *570*(June 2018), 692–704. <https://doi.org/10.1016/j.jhydrol.2018.12.043>
- Gao, X., Ge, D. B., Deng, Z. M., Xie, Y. H., & Gao, T. J. (2015). Survival Strategy in the Wetland Sedge *Carex brevicuspis* (Cyperaceae) in Response to Flood and Drought: Avoidance or Tolerance? *Annales Botanici Fennici*, *52*(5–6), 401–410.  
<https://doi.org/10.5735/085.052.0523>
- Glaeser, L. C., House, M., & Vitt, D. H. (2021). Reclaiming to brackish wetlands in the Alberta oil sands: Comparison of responses to sodium concentrations by *Carex atherodes* and *Carex aquatilis*. *Plants*, *10*(8), 1–13. <https://doi.org/10.3390/plants10081511>
- Graham, J. A., Hartsock, J. A., Vitt, D. H., Wieder, R. K., & Gibson, J. J. (2016). Linkages between spatio-temporal patterns of environmental factors and distribution of plant assemblages across a boreal peatland complex. *Boreas*, *45*(2), 207–219.  
<https://doi.org/10.1111/bor.12151>
- Guidi, L., Lo Piccolo, E., & Landi, M. (2019). Chlorophyll fluorescence, photoinhibition and abiotic stress: Does it make any difference the fact to be a C3 or C4 species? *Frontiers in Plant Science*, *10*(February), 1–11. <https://doi.org/10.3389/fpls.2019.00174>

- Hájek, M., Hájková, P., Kočí, M., Jiroušek, M., Mikulášková, E., & Kintrová, K. (2013). Do we need soil moisture measurements in the vegetation-environment studies in wetlands? *Journal of Vegetation Science*, 24(1), 127–137. <https://doi.org/10.1111/j.1654-1103.2012.01440.x>
- Huang, R., McPhedran, K. N., Yang, L., & Gamal El-Din, M. (2016). Characterization and distribution of metal and nonmetal elements in the Alberta oil sands region of Canada. *Chemosphere*, 147, 218–229. <https://doi.org/10.1016/j.chemosphere.2015.12.099>
- Irving, L. J. (2015). Carbon assimilation, biomass partitioning and productivity in grasses. *Agriculture (Pol'nohospodarstvo)*, 5(4), 1116–1134. <https://doi.org/10.3390/agriculture5041116>
- Jalal, A., Oliveira Junior, J. C. de, Ribeiro, J. S., Fernandes, G. C., Mariano, G. G., Trindade, V. D. R., & Reis, A. R. dos. (2021). Hormesis in plants: Physiological and biochemical responses. *Ecotoxicology and Environmental Safety*, 207(August 2020). <https://doi.org/10.1016/j.ecoenv.2020.111225>
- Jassey, V. E. J., & Signarbieux, C. (2019). Effects of climate warming on Sphagnum photosynthesis in peatlands depend on peat moisture and species-specific anatomical traits. *Global Change Biology*, 25(11), 3859–3870. <https://doi.org/10.1111/gcb.14788>
- Jiang, S., Tang, Y., Fan, R., Bai, S., Wang, X., Huang, Y., Li, W., & Ji, W. (2023). Response of *Carex breviculmis* to phosphorus deficiency and drought stress. *Frontiers in Plant Science*, 14(July), 1–18. <https://doi.org/10.3389/fpls.2023.1203924>
- Kennedy, G., & Mayer, T. (2002). Natural and constructed wetlands in Canada: An overview. *Water Quality Research Journal of Canada*, 37(2), 295–325. <https://doi.org/10.2166/wqrj.2002.020>

- Kessel, E. D., Ketcheson, S. J., & Price, J. S. (2018). The distribution and migration of sodium from a reclaimed upland to a constructed fen peatland in a post-mined oil sands landscape. *Science of the Total Environment*, *630*, 1553–1564.  
<https://doi.org/10.1016/j.scitotenv.2018.02.253>
- Ketcheson, S. J., Price, J. S., Carey, S. K., Petrone, R. M., Mendoza, C. A., & Devito, K. J. (2016). Constructing fen peatlands in post-mining oil sands landscapes: Challenges and opportunities from a hydrological perspective. *Earth-Science Reviews*, *161*(August), 130–139. <https://doi.org/10.1016/j.earscirev.2016.08.007>
- Kruskal, W. H. ;, & Wallis, W. A. (1989). Journal of the American Chemical. *Analytical Chemistry*, *61*(8), 564A-564A. <https://doi.org/10.1021/ac00183a752>
- Lai, W. L., Zhang, Y., & Chen, Z. H. (2012). Radial oxygen loss, photosynthesis, and nutrient removal of 35 wetland plants. *Ecological Engineering*, *39*, 24–30.  
<https://doi.org/10.1016/j.ecoleng.2011.11.010>
- Limpens, J., Berendse, F., Blodau, C., Canadell, J. G., Freeman, C., Holden, J., Roulet, N., Rydin, H., & Schaepman-Strub, G. (2008). Peatlands and the carbon cycle: From local processes to global implications - A synthesis. *Biogeosciences*, *5*(5), 1475–1491.  
<https://doi.org/10.5194/bg-5-1475-2008>
- Loreti, E., & Perata, P. (2020). The Many Facets of Hypoxia in Plants. *Plants*, *9*(6), 745.  
<https://doi.org/10.3390/plants9060745>
- Loreto, F., & Centritto, M. (2008). Leaf carbon assimilation in a water-limited world. *Plant Biosystems*, *142*(1), 154–161. <https://doi.org/10.1080/11263500701872937>
- Mainiero, R., & Kazda, M. (2005). Effects of *Carex rostrata* on soil oxygen in relation to soil moisture. *Plant and Soil*, *270*(1), 311–320. <https://doi.org/10.1007/s11104-004-1724-z>
- Maxwell, K., & Johnson, G. N. (2000). Chlorophyll fluorescence—a practical guide. *Journal of Experimental Botany*, *51*(345), 659–668. <https://doi.org/10.1016/j.rsci.2018.02.001>

- Mollard, F. P. O., Roy, M., Frederick, K., & Foote, L. (2012). Growth of the dominant macrophyte *Carex aquatilis* is inhibited in oil sands affected wetlands in Northern Alberta, Canada. *Ecological Engineering*, 38(1), 11–19.  
<https://doi.org/10.1016/j.ecoleng.2011.09.002>
- Muhammad Arslan Ashraf. (2012). Waterlogging stress in plants: A review. *African Journal of Agricultural Research*, 7(13), 1976–1981. <https://doi.org/10.5897/ajarx11.084>
- Munns, R. (2002). Comparative physiology of salt and water stress. *Plant, Cell and Environment*, 25(2), 239–250. <https://doi.org/10.1046/j.0016-8025.2001.00808.x>
- Munns, R., & Tester, M. (2008). Mechanisms of salinity tolerance. *Annual Review of Plant Biology*, 59, 651–681. <https://doi.org/10.1146/annurev.arplant.59.032607.092911>
- Murchie, E. H., & Lawson, T. (2013). Chlorophyll fluorescence analysis: A guide to good practice and understanding some new applications. *Journal of Experimental Botany*, 64(13), 3983–3998. <https://doi.org/10.1093/jxb/ert208>
- Murray, K. R., Barlow, N., & Strack, M. (2017). Methane emissions dynamics from a constructed fen and reference sites in the Athabasca Oil Sands Region, Alberta. *Science of the Total Environment*, 583, 369–381. <https://doi.org/10.1016/j.scitotenv.2017.01.076>
- Nilson, S. E., & Assmann, S. M. (2007). The control of transpiration. Insights from arabidopsis. *Plant Physiology*, 143(1), 19–27. <https://doi.org/10.1104/pp.106.093161>
- Olvera-González, E., Alaniz-Lumbreras, D., Ivanov-Tsonchev, R., Villa-Hernández, J., de la Rosa-Vargas, I., López-Cruz, I., Silos-Espino, H., & Lara-Herrera, A. (2013). Chlorophyll fluorescence emission of tomato plants as a response to pulsed light based LEDs. *Plant Growth Regulation*, 69(2), 117–123. <https://doi.org/10.1007/s10725-012-9753-8>

- Popović, N., Petrone, R. M., Green, A., Khomik, M., & Price, J. S. (2022). A temporal snapshot of ecosystem functionality during the initial stages of reclamation of an upland-fen complex. *Journal of Hydrology: Regional Studies*, 41(March).  
<https://doi.org/10.1016/j.ejrh.2022.101078>
- Potvin, L. R., Kane, E. S., Chimner, R. A., Kolka, R. K., & Lilleskov, E. A. (2015). Effects of water table position and plant functional group on plant community, aboveground production, and peat properties in a peatland mesocosm experiment (PEATcosm). *Plant and Soil*, 387(1–2), 277–294. <https://doi.org/10.1007/s11104-014-2301-8>
- Price, J. S., McLaren, R. G., & Rudolph, D. L. (2010). Landscape restoration after oil sands mining: Conceptual design and hydrological modelling for fen reconstruction. *International Journal of Mining, Reclamation and Environment*, 24(2), 109–123.  
<https://doi.org/10.1080/17480930902955724>
- Purdy, B. G., Macdonald, S. E., & Lieffers, V. J. (2005). Naturally saline boreal communities as models for reclamation of saline oil sand tailings. *Restoration Ecology*, 13(4), 667–677. <https://doi.org/10.1111/j.1526-100X.2005.00085.x>
- Reavis, M., Purcell, L. C., Pereira, A., & Naithani, K. (2023). Effects of measurement methods and growing conditions on phenotypic expression of photosynthesis in seven diverse rice genotypes. *Frontiers in Plant Science*, 14(September), 1–10.  
<https://doi.org/10.3389/fpls.2023.1106672>
- Rooney, R. C., & Bayley, S. E. (2011). Setting reclamation targets and evaluating progress: Submersed aquatic vegetation in natural and post-oil sands mining wetlands in Alberta, Canada. *Ecological Engineering*, 37(4), 569–579.  
<https://doi.org/10.1016/j.ecoleng.2010.11.032>
- Siegel, S. (1957). Nonparametric Statistics. *American Statistician*, 11(3), 13–19.  
<https://doi.org/10.1080/00031305.1957.10501091>

- Sorrell, B. K., Tanner, C. C., & Brix, H. (2012). Regression analysis of growth responses to water depth in three wetland plant species. *AoB Plants*, 2012(0), pls043–pls043. <https://doi.org/10.1093/aobpla/pls043>
- Strack, M., Keith, A. M., & Xu, B. (2014). Growing season carbon dioxide and methane exchange at a restored peatland on the Western Boreal Plain. *Ecological Engineering*, 64, 231–239. <https://doi.org/10.1016/j.ecoleng.2013.12.013>
- Sutton, O. F., & Price, J. S. (2020). Modelling the hydrologic effects of vegetation growth on the long-term trajectory of a reclamation watershed. *Science of the Total Environment*, 734, 139323. <https://doi.org/10.1016/j.scitotenv.2020.139323>
- Thompson, C., Mendoza, C. A., & Devito, K. J. (2017). Potential influence of climate change on ecosystems within the Boreal Plains of Alberta. *Hydrological Processes*, 31(11), 2110–2124. <https://doi.org/10.1002/hyp.11183>
- Trites, M., & Bayley, S. E. (2009). Vegetation communities in continental boreal wetlands along a salinity gradient: Implications for oil sands mining reclamation. *Aquatic Botany*, 91(1), 27–39. <https://doi.org/10.1016/j.aquabot.2009.01.003>
- Vitt, D. H., Glaeser, L. C., House, M., & Kitchen, S. P. (2020). Structural and functional responses of *Carex aquatilis* to increasing sodium concentrations. *Wetlands Ecology and Management*, 28(5), 753–763. <https://doi.org/10.1007/s11273-020-09746-9>
- Vitt, D. H., Wieder, R. K., Xu, B., Kaskie, M., & Koropchak, S. (2011). Peatland establishment on mineral soils: Effects of water level, amendments, and species after two growing seasons. *Ecological Engineering*, 37(2), 354–363. <https://doi.org/10.1016/j.ecoleng.2010.11.029>

Volik, O., Elmes, M., Petrone, R., Kessel, E., Green, A., Cobbaert, D., & Price, J. (2020).

Wetlands in the athabasca oil sands region: The nexus between wetland hydrological function and resource extraction. *Environmental Reviews*, 28(3), 246–261.

<https://doi.org/10.1139/er-2019-0040>

Volik, O., Petrone, R. M., Quanz, M., Macrae, M. L., Rooney, R., & Price, J. S. (2020).

Environmental Controls on CO<sub>2</sub> Exchange along a Salinity Gradient in a Saline Boreal Fen in the Athabasca Oil Sands Region. *Wetlands*, 40(5), 1353–1366.

<https://doi.org/10.1007/s13157-019-01257-5>

Volik, O., Petrone, R. M., Wells, C. M., & Price, J. S. (2018). Impact of Salinity, Hydrology and Vegetation on Long-Term Carbon Accumulation in a Saline Boreal Peatland and its

Implication for Peatland Reclamation in the Athabasca Oil Sands Region. *Wetlands*,

38(2), 373–382. <https://doi.org/10.1007/s13157-017-0974-5>

Wells, C. M., & Price, J. S. (2015). A hydrologic assessment of a saline-spring fen in the

Athabasca oil sands region, Alberta, Canada - a potential analogue for oil sands reclamation. *Hydrological Processes*, 29(20), 4533–4548.

<https://doi.org/10.1002/hyp.10518>

Were, D., Kansime, F., Fetahi, T., Cooper, A., & Jjuuko, C. (2019). Carbon Sequestration by

Wetlands: A Critical Review of Enhancement Measures for Climate Change Mitigation.

*Earth Systems and Environment*, 3(2), 327–340. [https://doi.org/10.1007/s41748-019-](https://doi.org/10.1007/s41748-019-00094-0)

[00094-0](https://doi.org/10.1007/s41748-019-00094-0)

Xia, Q., Tang, H., Fu, L., Tan, J., Govindjee, G., & Guo, Y. (2023). Determination of Fv/Fm

from Chlorophyll a Fluorescence without Dark Adaptation by an LSSVM Model. *Plant*

*Phenomics*, 5, 1–11. <https://doi.org/10.34133/plantphenomics.0034>

- Yang, S., Sutton, O. F., Kessel, E. D., & Price, J. S. (2022). Spatial patterns and mass balance of sodium in near-surface peat of a constructed fen. *Journal of Hydrology: Regional Studies*, 41(April), 101073. <https://doi.org/10.1016/j.ejrh.2022.101073>
- Yao, X., Cao, Y., Zheng, G., Devlin, A. T., Li, X., Li, M., Tang, S., & Xu, L. (2021). Ecological adaptability and population growth tolerance characteristics of *Carex cinerascens* in response to water level changes in Poyang Lake, China. *Scientific Reports*, 11(1), 1–15. <https://doi.org/10.1038/s41598-021-84282-x>
- Zhang, D., Zhang, M., Tong, S., Qi, Q., Wang, X., & Lu, X. (2020). Growth and physiological response of *Carex schmidtii* to water-level fluctuation. *Hydrobiologia*, 847(3), 967–981. <https://doi.org/10.1007/s10750-019-04159-z>
- Zhong, Y., Jiang, M., & Middleton, B. A. (2020). Effects of water level alteration on carbon cycling in peatlands. *Ecosystem Health and Sustainability*, 6(1). <https://doi.org/10.1080/20964129.2020.1806113>
- Zhou, Z., Su, P., Wu, X., Shi, R., & Ding, X. (2021). Leaf and Community Photosynthetic Carbon Assimilation of Alpine Plants Under in-situ Warming. *Frontiers in Plant Science*, 12(July). <https://doi.org/10.3389/fpls.2021.690077>